



The operational role of remote sensing in assessing and predicting land use/land cover and seasonal land surface temperature using machine learning algorithms in Rajshahi, Bangladesh

Abdulla - Al Kafy^{1,2} · Abdullah-Al-Faisal^{1,3} · Abdullah Al Rakib¹ · Kaniz Shaleha Akter¹ · Zullyadini A. Rahaman⁴ · Dewan Md. Amir Jahir¹ · Gangaraju Subramanyam⁵ · Opelele Omeno Michel⁶ · Abhishek Bhatt⁷

Received: 12 August 2020 / Accepted: 22 July 2021 / Published online: 24 August 2021
© Società Italiana di Fotogrammetria e Topografia (SIFET) 2021

Abstract

Human activity has boosted carbon dioxide emissions, causing temperatures to rise. The average temperature on Earth is roughly 15 °C, but it has been much higher and lower in the past. There are natural climatic changes, but experts say temperatures are already rising faster than at any other period in history. Unplanned urbanization can sometimes backfire, causing negative consequences that harm the economy and contribute to environmental damages, especially in developing countries like Bangladesh. Because of the strong association between land use/land cover and land surface temperature (LST), the study attempted to analyze and estimate LULC and seasonal (both summer and winter) LSTs using Landsat satellite images at 5-year intervals from 1995 to 2020. Later, the study forecasted both LULC and seasonal LSTs for 2030 and 2040 using cellular automata (CA) and artificial neural network (ANN) algorithms for Rajshahi district. As supporting parameters for determining the magnitude of climate change effects owing to urbanization and temperature rise, primary data collection procedures such as focus group discussions (FGDs) and key informant interviews (KIIs) with experts from diverse sectors were used. Results reveal that the built-up area was increased from 158.22 km² (6.64%) to 386.74 km² (16.23%) in this 25 years' timeframe, and it contributed the highest average temperature (41.68 °C in 2020 in summer) comparing with other LULCs. The LSTs were increasing at an alarming rate with 1–2 °C standard deviations per 5 years and maximum temperature was increased from 1995 to 2020 by 37.22 to 42.7 °C in summer and 22.18 to 28.94 °C in winter. Prediction states that net increase of built-up area will be 2.51 and 5.29, respectively, in 2030 and 2050 from 2020. Maximum LST will likely to be increased to 43.23 °C (2030) and 45.92 °C (2040) in summer, and 30.94 °C (2030) and 31.77 °C (2040) in winter. FGDs and KIIs assessments indicate that frequent LULC change was the main reason for increasing LSTs (71%) and 76% experts agreed that heat waves are the most influencing factors for adverse climate change, among other parameters. The work introduces new methods for integrating remote sensing data with primary datasets, which will provide substantial insights to urban planners and policymakers in terms of participatory and sustainable planning.

Keywords Urbanization · Land surface temperature · Cellular automata · Artificial neural network · Participatory planning

✉ Zullyadini A. Rahaman
zully@fsk.upsi.edu.my

Abdulla - Al Kafy
abdulla-al.kafy@localpathways.org

¹ Department of Urban & Regional Planning, Rajshahi University of Engineering & Technology (RUET), Rajshahi 6204, Bangladesh

² ICLEI South Asia, Rajshahi City Corporation, Rajshahi 6203, Bangladesh

³ GIS Centre, Operational Centre Amsterdam (OCA), Médecins Sans Frontières (MSF), Cox's Bazar 4750, Bangladesh

⁴ Department of Geography & Environment, Faculty of Human Sciences, Sultan Idris Education University, 35900 Tanjung Malim, Malaysia

⁵ Regional Agricultural Research Station, Tirupati, India

⁶ Département de Natural Resources Management, Faculty of Agricultural Sciences, University of Kinshasa, Kinshasa, Democratic Republic of Congo

⁷ Department of Electronics and Telecommunication, College of Engineering, Pune, India

Introduction

Urbanization is the process by which large populations become permanently concentrated in relatively small regions, resulting in the formation of cities. It is also the process through which cities develop and an increasing proportion of the population resides and migrates in cities. However, in the modern world, urbanization is becoming a headache for every country's urban planner and policy makers. Haphazard urban growth and unplanned expansion of urban areas are common scenarios in almost all developing countries, especially in South Asia. Today, 50% of the world's total population is urbanized, which is expected to reach 68% by 2050 (Habitat 2016; Kafy et al. 2019). Rapid and uncontrolled urban migration, the concentration of better jobs in city areas, and discrimination in the placement of civic facilities are among the major reasons behind the massive flow of urban migration. Modern urban development accelerates urbanization that pressures modern cities and affects the surrounding environment, ecosystem, and biodiversity (Al Rakib et al. 2020a; Chakroborty et al. 2020; Kafy et al. 2021a, 2020b; Rahman et al. 2018). Urban areas sometimes act as a ceaseless platform of various economic activities and local–regional development, by representing more than 54% of the worldwide population (Al Rakib et al. 2020b; Dey et al. 2021; Ullah et al. 2019a). Though urbanization is an indicator of economic progress and social and technological advancement of a city, it certainly creates many short and long-term demerits in various aspects (Celik et al. 2019; Maimaitiyiming et al. 2014). A rapid change in land cover creating a vast effect in the increment of land surface temperature (LST) with hampering the climate and ecological balance is one of the significant long-term consequences of modern urbanization (Kafy et al. 2020b; Maimaitiyiming et al. 2014; Mallik et al. 2008). Land cover changes are considered one of the leading causes behind the rising temperature in cities that is fueled by the urban consumption of cool land covers, i.e., vegetated and agricultural surfaces, wetlands, and water bodies (Halmy et al. 2015; Kafy et al. 2020b; Mishra and Rai 2016; Pal and Ziaul 2017; Zhou et al. 2011; Zine El Abidine et al. 2014). Land use usually refers to area which is localized and used by humans for various purposes and land cover means area with natural surfaces and resources of land but they are regularly studied together for having strong correlation with each other (Al Rakib et al. 2020a; Verburg et al. 2009). Over the years, a significant shift in built-up and urban areas is noticed as only 3% of urban areas worldwide in 1950 and is expected to reach 66% by 2050 (UN-DESA 2018). This increasing trend has a drastic effect on the surrounding environment and climate, as urban areas have 2–4 °C more temperature

than the rural areas and surrounding land use/land cover (LU/LC) (Lai and Cheng 2010). Numerous factors like reluctance in vertical urban growth, construction materials, short distance between buildings and infrastructures, unplanned placement of public squares, roads, highways, short and large industrial hub, and commercial concentration are responsible for the constant upsurge in temperature (Ahmed et al. 2013; Chen et al. 2006; Dey et al. 2021; Durand et al. 2011; Kafy et al. 2020b, 2021c; Pal and Ziaul 2017). This increasing trend and consumption of cool land covers result in the urban heat island (UHI) creation in major urban centers worldwide (Ahmed 2018; Kafy et al. 2020c; Naim and Kafy 2021; Yang et al. 2017) that has a higher connectivity with high energy consumption, surrounding air quality, and health risks for humans such as cancer, and respiratory illness (Ahmed et al. 2013; Ogashawara and Bastos 2012; Pal and Ziaul 2017). Mitigating the formation of these UHIs can be achieved by the implementation of systematic and planned approach taken by urban planners for the betterment of living environments, human health, and surrounding nature.

Different satellite data are used to examine the LULC change dynamics such as Landsat, SPOT, Sentinel, and MODIS data (Al-Hamdan et al. 2017; Halmy et al. 2015; Kafy et al. 2021b; McCarthy et al. 2018; Osgouei and Kaya 2017). Hence, the Landsat satellite data is often used by researchers for its high availability, good temporal resolution, free-access, and long-range time-series data (Dey et al. 2021; Lu et al. 2019). The integrated approach of Geographic Information System (GIS) and Remote Sensing (RS) is greatly considered among researchers to measure the LULC change dynamics and spatiotemporal distribution of LST (Al Rakib et al. 2020a; Balogun and Ishola 2017; Dey et al. 2021; Faisal et al. 2021; Kafy et al. 2020b, 2021d; Lily Rose and Devadas 2009; Rahman et al. 2018). LULC change detection and LST monitoring through field visits are time-consuming, error-prone, and highly labor-intensive (Hart and Sailor 2009; Lily Rose and Devadas 2009). Meanwhile, the integrated approach of GIS and RS technology is more user-friendly, technologically advanced, and more efficiently examine, monitor, and map the LULC and LST change (Fu and Weng 2018; Niyogi 2019; Trolle et al. 2019). Statistical and technological advancements in numerous methods using diverse satellite data have influenced spatiotemporal modeling of LULC and LST change and resulted in efficient solutions to difficulties associated with this phenomenon (Ahmed et al. 2013; Celik et al. 2019; Faisal et al. 2021; Fu and Weng 2018; Gaur et al. 2018; Rahman 2016; Zine El Abidine et al. 2014). Researchers worldwide have also analyzed the spatial distribution of LST on different LULC classes using available thermal sensors to better understand the influence of LULC change on LST (Celik et al. 2019; Rahman et al. 2017a, b).

To understand the dynamics of one area, evaluation of LULC change and their impact on spatiotemporal LST distribution is not enough. However, predicting the future LULC and LST scenarios and the effects of the current changing pattern is also needed to better understand the impact of this phenomenon. Predicted LULC and LST change scenario are playing a crucial role in decision-making and policy improvement as it provides the decision-makers and urban planners with a better view of the future needs and impact of the present trends (Handayanto et al. 2017; Kafy et al. 2021d; UN “Sustainable Development Goals” 2015). As the LULC and LST change prediction is spatial in nature, researchers need a comprehensive strategic approach to predict the future scenarios (Kafy et al. 2020b). Researchers worldwide took various approaches to predict the future scenario like Markov Chain (MC) (Guan et al. 2011), Cellular Automata (CA) (Al sharif and Pradhan 2014; Kafy et al. 2021e), Multi-Layer Perception Markov Chain (MLP—MC) (Arsanjani et al. 2013; Mishra and Rai 2016), Artificial Neural Network (ANN) (Azari et al. 2016; Maduako et al. 2016a, b; Mozumder and Tripathi 2014), Cellular Automata—Markov (CA—Markov) chain (Ghosh et al. 2017; Islam et al. 2018), Binary Logistic Regression algorithm (Liu et al. 2017), and CLUE (Singh et al. 2015) models. All the prediction models have their own algorithms and methodology to perform the simulation. Among them, the CA model uses the previous cell values within a neighborhood to predict according to a series of transition rules (Al sharif and Pradhan 2014; Pal and Ziaul 2017). On the other hand, the ANN is inspired by the human brain’s nerve system that evaluates and models the non-linear trends (Kafy et al. 2020c; Maduako et al. 2016a, b). The MLP-MC model was recently developed, integrating the Multi-Layer Perception Neural Network (MLP-NN) and MC model (Fortin et al. 2003). It takes a qualitative LULC map of two consecutive years as input and produces a transition matrix (Kafy et al. 2020b; Maduako et al. 2016a, b; Mishra et al. 2018; Mishra and Rai 2016). This model also suggests a scenario that a raster unit (pixel) will convert to one category of LULC from another within a certain time period based on the past trends (Eastman 2012). The MC model is also a known method to understand and simulate the landscape changes (Al sharif and Pradhan 2014). But this model is recommended for the areas for which the LULC change pattern is known (Maithani 2015). The MC also extracts the LULC conversion area to simulate the transition pattern (Kafy et al. 2020b). Despite all the advantages, MLP-MC method takes precedence over MLP-NN and MC for its advanced algorithm, higher accuracy, and the best possible simulation of urban expansion (Dey et al. 2021; Mishra et al. 2018).

In recent times, several methods are applied by researchers to predict the LULC and LST change dynamics for their respective study areas (Al sharif and Pradhan 2014; Celik

et al. 2019; Kafy et al. 2021e; Mishra et al. 2018). Mishra et al. (2018) examined and compared the application of Stochastic Markov Chain (ST—MC), MLP-MC, and CA models to examine and predict the future LULC scenario of Varanasi, India (Mishra et al. 2018). Kafy et al. (2021e) used CA model to predict the future LULC dynamics of Dhaka Metropolitan Area with high-resolution RapidEye satellite images that showed a high level of accuracy (Kafy et al. 2021e). Zine El Abidine et al. (2014) correlated the relation between LULC and LST dynamics and used that to model urban heat waves in Middle Eastern cities (Zine El Abidine et al. 2014).

Rajshahi district, located in Bangladesh’s northeastern region, is an agricultural-based region that is well-connected throughout the country. Better living standards, access to better educational institutions, and employment opportunities have attracted people towards Rajshahi over the past few decades. The increasing population pressure is accelerating unplanned infrastructural development in this region. Methods incorporating CA and ANN algorithms have the potential to yield valuable insights into the short and long-term consequences of LULC and LST change in this region. It can also help the decision-makers and urban planners to reduce the effect of UHI. The current study is a regional scale study and the first of its kind in Bangladesh’s northwest region, intending to determine the past (1995, 2000, 2005, 2010, 2015, and 2020) and future (2030 and 2040) trend of LULC and seasonal (summer and winter) LST change, as well as LST variation across different LULC classes, using novel approaches such as support vector machine (SVM), CA, and ANN algorithms. Finally, this study engages the local community people and professionals through Focus Group Discussions (FGDs) and Key Informant Interviews (KIIs) to identify the impact of LULC, seasonal LST, and climate change in the study region for developing sustainable land use management, temperature increase, and climate change mitigating strategies. This study will be an effective tool for urban planners and policymakers to understand the LULC change and its impact on seasonal LST distribution in a more comprehensive manner.

Study area profile

Rajshahi district, the divisional center-point of Rajshahi Division, is situated in the north-western part of Bangladesh, standing upon the northern bank of the Padma River. It lies between 24° 12’ N to 24° 44’ N latitude and 88° 18’ E to 88° 58’ E longitude (Fig. 1). This region serves as one of Bangladesh’s most influential commercial and educational cores, with an approximate area of about 2428 km² (BBS 2013; Clemett et al. 2006; RDA 2008). Though the majority portion of the Rajshahi district serves the agricultural

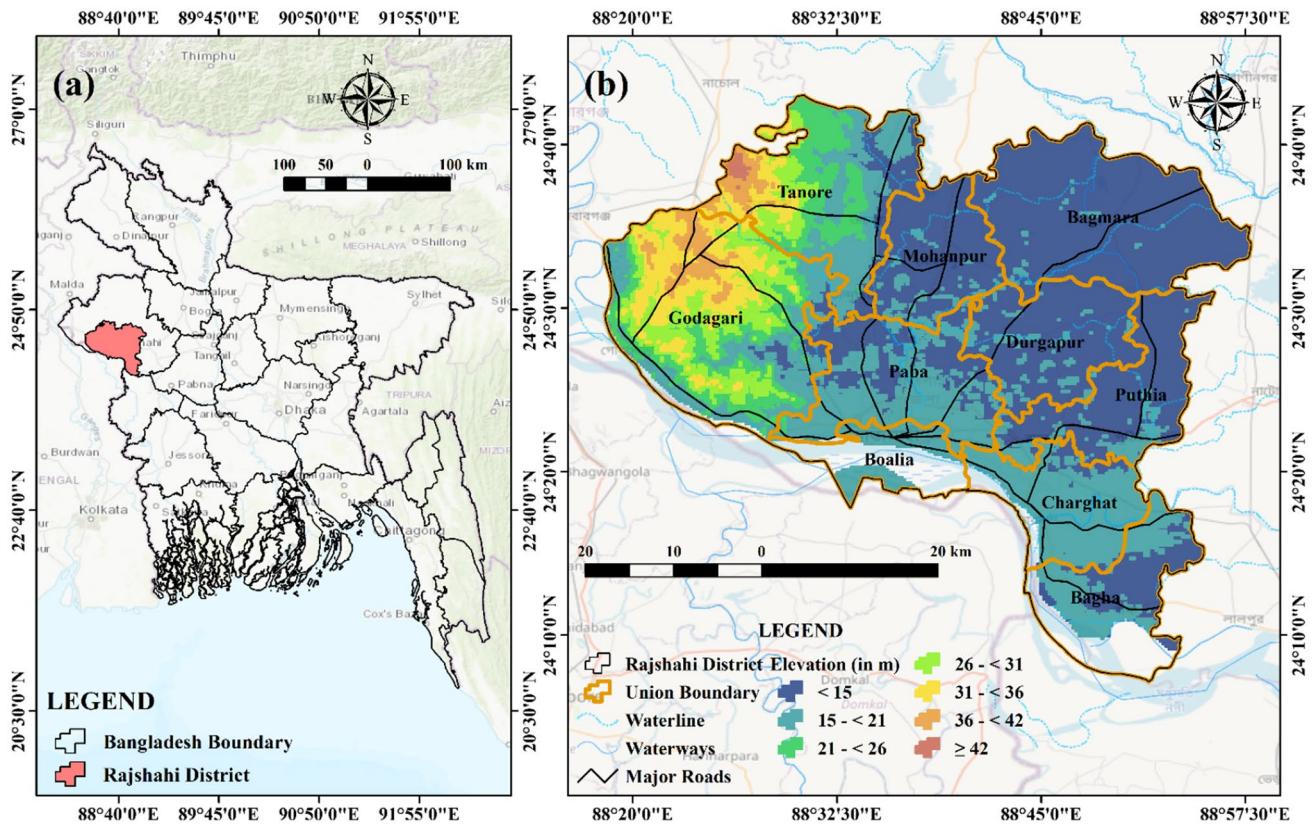


Fig. 1 Location map of the study area. **a** Rajshahi district in Bangladesh. **b** Rajshahi district

purpose, this area is continuously exposed to uncontrolled and unmonitored urbanization since the beginning of the twenty-first century. This haphazard development resulted in a reduction of 14% of vegetation and agricultural land with an increment of infrastructure development by 19.4% from 1997 to 2010 (Islam and Hassan 2012). By the next decade, Rajshahi district had only 43.12% of the total area consisting of agricultural land and vegetation, 32.13% of bare land, 14.17% of built-up area, and 10.58% of water bodies (Kafy et al. 2020a). The unplanned and uncontrolled transition between different LULCs negatively influences the ecological sustainability of an area, as this transition significantly replaces cool land covers like vegetation, agricultural land, and water bodies to built-up areas. City-level studies have shown that the haphazard urban growth with uncontrolled depletion of cool land covers significantly accelerates the rise in LST (Kafy et al. 2020a).

The climate of the Rajshahi district is divided into different monsoons that brings moderate rainfall, high humidity, and escalating temperature. Four distinctive seasons are noticed in this region, i.e., winter (low rainfall, temperature, and humidity) from October to February; summer (low rainfall, high temperature, and humidity) from March to June; and monsoon (heavy rainfall, moderate

temperature, humidity) from July to September (Alamgir et al. 2020). Higher temperature is varying between 30 and 40 °C and usually remains in mid-summer, i.e., April and May. On the other hand, the lower temperature is varying between 18 and 23 °C and generally remnants in mid-winter, i.e., December and January (BBS 2013; Kafy et al. 2020b; UN 2019).

Despite being an agrarian region, a pick level industrialization has occurred in this region after the opening of Jamuna Bridge in 1998 (Amzad Hossain 2017; Wadud 2018). The huge urban influx was seen in this region due to major urban migration which was tremendously affected by better life opportunity and abundant job opportunities (Al Rakib et al. 2020c; Kafy et al. 2019). In 2001, this region consisted of a total population of 22,86,874, having a population density of 941 people/km² (BBS 2013; Clemett et al. 2006). By 2016, the total population of this region was increased to 28,53,000 with a population density of 1175 people/km² (BBS 2013; UN 2019). Unregulated urbanization and haphazard consumption of different LULCs highly impacted the seasonal severity of this region in the last few years that greatly affected biodiversity, ecology, livelihood, and agricultural development (Kafy et al. 2020a).

Data and methodology

Data description

Both primary and secondary datasets were used for this study. The study period was set to be the years 1995, 2000, 2005, 2010, 2015, and 2020. Over this silver jubilee, twelve sets of multispectral Landsat satellite data were acquired from United States Geological Survey (USGS) to examine the LULC change in the study area and its impact on the seasonal LST distribution. All of the images were collected for both the summer and winter seasons, where April was considered for summer and December was considered for the winter season. Cloud cover was set to < 10%, though all the images had nearly 0% cloud cover over the study region. The images had a spatial resolution of 30 m. Preprocessing stage of the images was avoided as Landsat satellite data is free from radiometric and geometric distortion (Kafy et al. 2021d). A detailed description of the acquired data is shown in Table 1.

Primary data collection

Primary data was collected by conducting a field visit in February 2020. Global Positioning System (GPS) was used to assemble the ground truth data for the accuracy assessment of classified LULC maps for the year 2020. Ten FGDs and

twenty KIIs were conducted from January 2020 to March 2020 to identify the possible impacts of LULC change, seasonal LST shifts, and climate change in the study area. The FGDs will help to identify the impacts of LULC and temperature changes on the study area in the last 25 years. The KIIs with experts will assist in identifying the possible impacts of climate change on the study region. Based on the suggestions provided by the FGD and KII participants, strategies for ensuring sustainable land use management, reducing the temperature increase, and mitigate the climate change impacts have been developed. The FGDs were conducted in ten unions of the Rajshahi district (Fig. 1b). The KIIs and FGDs (8–10 participants) assessments were consisted of urban planners, agricultural officers, environmental engineers, policymakers, local community leaders, and decision-makers. The outputs from FGDs and KIIs has been discussed in the “Impact on LULC, seasonal LST, and climate change based on KIIs and FGDs” section.

Classification of LULC map

All the acquired images were classified into four major LULC class, i.e., water bodies, built-up area, agricultural land, and bare land for the whole study period using a support vector machine (SVM) algorithm in ENVI 5.3 software. A detailed description of each LULC is provided in Table 2. The SVM algorithm is a powerful LULC classification method as it is derived from statistical learning

Table 1 Description of the collected Landsat data from USGS

Year	Season	Acquired date	Path/row	Sensor	Spatial resolution	Cloud cover
1995	Summer	18 April 1995	138/043	Landsat 5 TM	30 m	< 10%
	Winter	28 November 1995				
2000	Summer	15 April 2000				
	Winter	11 December 2000				
2005	Summer	13 April 2005				
	Winter	7 November 2005				
2010	Summer	11 April 2010				
	Winter	23 December 2010				
2015	Summer	9 April 2015			Landsat 8 OLI	
	Winter	21 December 2015				
2020	Summer	6 April 2020				
	Winter	18 December 2020				

Table 2 Description of features in each LULC

Land cover	Covered land use and features
Built-up area	Residential, industrial, functional areas, impervious layers, and transportation network
Agricultural land	All types of vegetation, herb, shrubs, cultivation, and agricultural lands
Water bodies	Rivers, wetlands, ponds, water reservoirs, canals, and streams
Bare land	Fallow land, sand, large playground, open ground, and landfill sites

theory that usually produces more accuracy in the classified images even if the data is complex and noisy (Maulik and Chakraborty 2017). Survey data, background information, and local knowledge on existing and previous LULC classes were considered to ensure the maximum accuracy of the signature data used in the image classification.

Classification accuracy assessment

A total of 1800 ground-truthing points were collected from 6 years of images using random sampling technique. The same number of points were used to validate the accuracy of the classified maps using points collected from the Google earth platform (GEP) and GPS. A total of 300 points were collected from the GEP for each year from 1995 to 2015. For the year 2020, 200 points were collected using GPS during the field visit and 100 points were collected from GEP. Overall accuracy, User accuracy, Producers' accuracy, and Kappa statistics were calculated using the equations shown in Table 3, which are considered one of the best classification accuracy assessment techniques (Rahman et al. 2018).

Estimation of seasonal LST

Spatial distribution of seasonal (summer and winter) LST during the study period (1995–2020) was evaluated using Landsat thermal bands from the acquired datasets. Landsat thermal sensor acquires thermal data as Digital Number (DN) that were converted to LST using the equations which are shown in Fig. 2 (Celik et al. 2019; Connors et al. 2013; Maduako et al. 2016a, b; Pal and Ziaul 2017; Shatnawi and Abu Qdais 2019; Ullah et al. 2019b).

Seasonal LST variation over different LULC classes

To evaluate the seasonal mean temperature variations over different LULC classes, the “Zonal Statistics” tool was used. An output table was generated by using zonal statistics showing the mean values of seasonal LST for each LULC class in ArcGIS 10.6 software. The “Zonal Statistics as Table” tool summarizes the mean temperature values within each class of LULC dataset and reports the results to a table (Fig. 3).

Prediction of temporal LULC change

The CA model was used to identify the future LULC change using QGIS's (version 3.18) MOLUSCE plugin as it considers all the static and dynamic aspects of change in every LULC categories with excellent accuracy (Al-sharif and Pradhan 2015; Balogun and Ishola 2017; Losiri et al. 2016; Santé et al. 2010). For using the MOLUSCE 3.0.13 version in the updated QGIS version, up-gradation of the freely available plugin python script was performed by keeping all the parameters same for prediction future LULC. As the model considers dependent and independent variables, elevation, slope, distance from the road network, water bodies, education institutions, and commercial areas were used as dependent variables and classified LULC maps for the study period were used as independent variables. Shapefiles of road networks, water bodies, education institutions, and commercial areas were collected from open street map platform to estimate the distance using the Euclidian distance function in ArcGIS 10.6 software. Digital Elevation—Shuttle Radar Topography Mission (SRTM) was used to calculate the elevation and slope characteristics. The estimated dependent variables developed a transition matrix using a random sampling technique by setting a maximum iteration of 1000 cells (3 × 3) neighborhood pixels. After developing the transition matrix, the CA model predicted future LULC maps for 2030 and 2040 in QGIS software. Before the prediction process for the years 2030 and 2040, the model was validated by predicting the LULC map for 2020 with a side-by-side comparison with the classified maps of the respective year. Multiple Kappa (K) parameters like $K_{location}$, K_{no} , $K_{location\ strata}$, and $K_{standard}$ were estimated in TerrSet software to validate and evaluate the model's accuracy level. The validation module of QGIS was also applied to examine the classification accuracy with Kappa coefficients comparing the classified maps and the predicted maps of the same years. The overall detailed classification and prediction procedures are given in Fig. 4.

LST prediction process for 2030 and 2040

The ANN algorithm in MATLAB software was used to predict the 2030 and 2040 seasonal LST scenarios. It is considered an effective approach in time-series prediction

Table 3 Equations used for classification accuracy assessment

Features	Equation
Overall accuracy	$\frac{\text{Total number of corrected classified pixels (diagonal)}}{\text{total number of reference pixels}} \times 100$
User accuracy	$\frac{\text{number of correctly classified pixels in each category (diagonal)}}{\text{total number of reference pixels in each category (row total)}} \times 100$
Producers' accuracy	$\frac{\text{number of correctly classified pixels in each category (diagonal)}}{\text{total number of reference pixels in each category (column total)}} \times 100$
Kappa coefficient	$\frac{\text{Total number of Sample} \times \text{Total Number of Corrected Sample} - \sum (\text{col.tot} \times \text{row tot})}{(\text{Total number of Sample})^2 - \sum (\text{col.tot} \times \text{row tot})} \times 100$



Fig. 2 Process of seasonal LST estimation using Landsat thermal bands

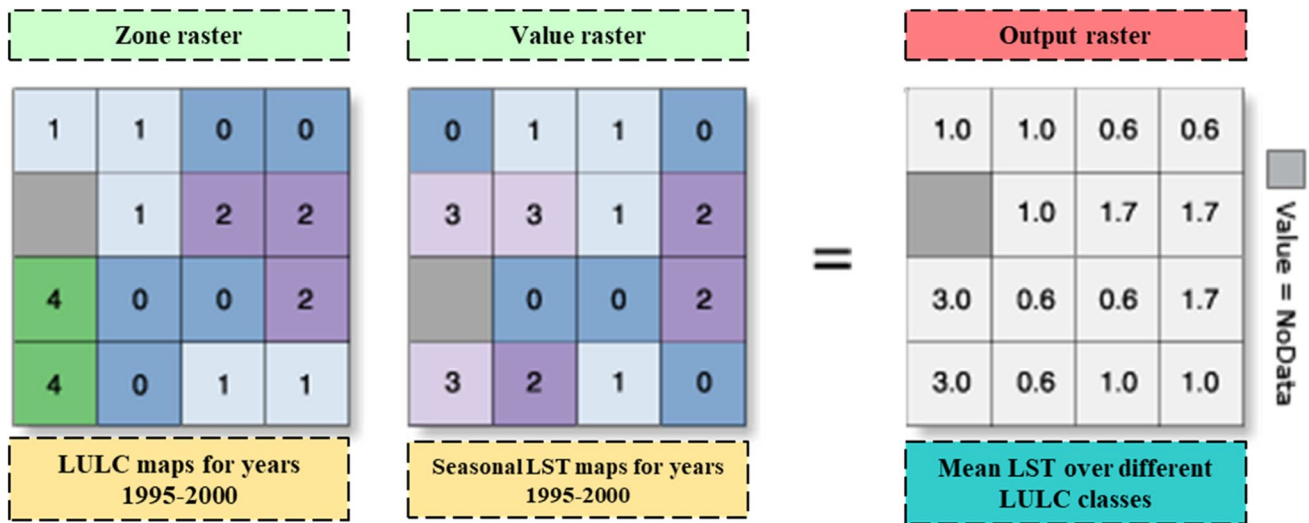


Fig. 3 Process of Zonal Statistics as Table in ArcGIS 10.6 software

using the previous years’ datasets (Faisal et al. 2021; Mas and Flores 2008; Shatnawi and Abu Qdais 2019). Firstly, the ANN algorithm creates a random output with a low

accuracy upon receiving the patterns. Then, the ANN algorithm computes the gap between the low accurate output and the intended output, which is a self-computed feature. Using

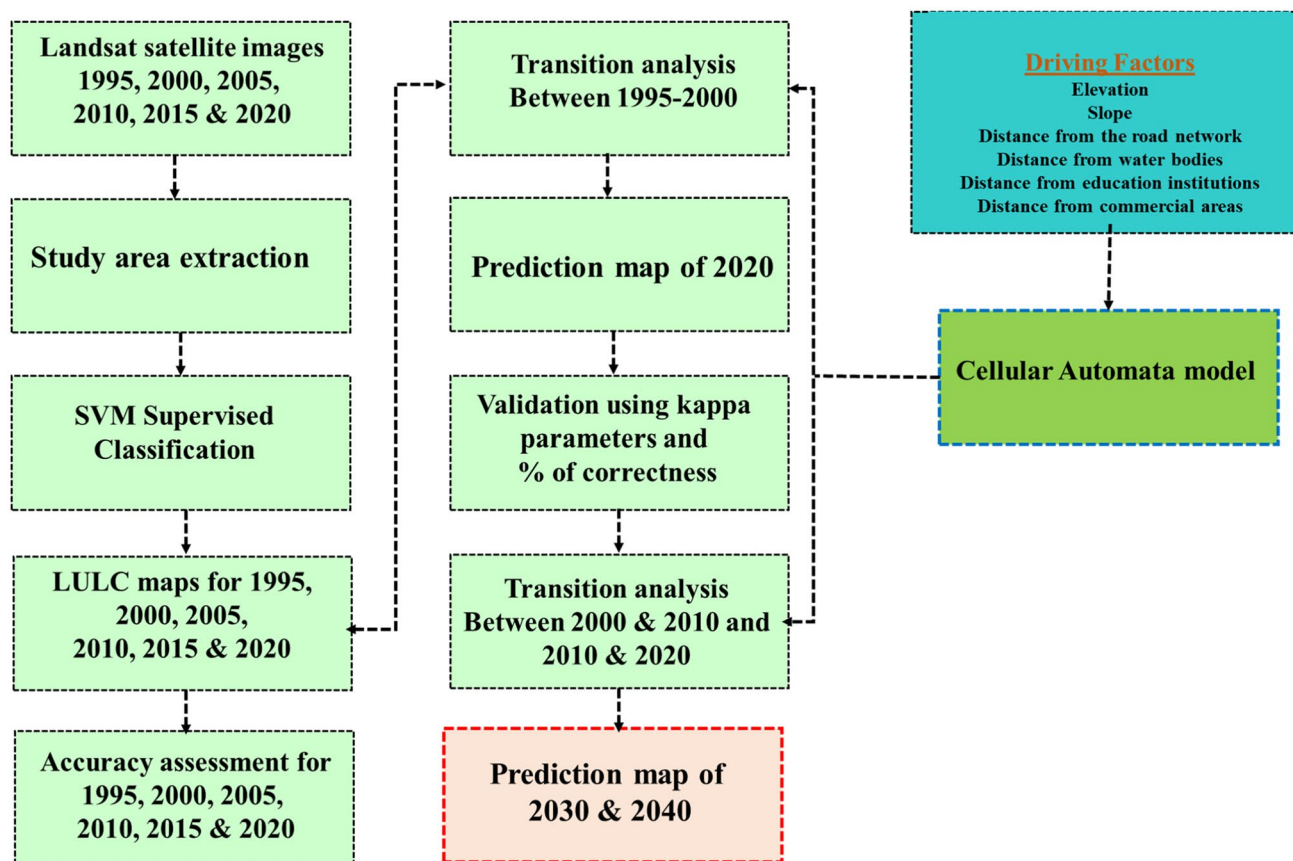


Fig. 4 Flowchart of LULC prediction process using CA algorithm

the “Leveraging backpropagation” algorithm, a correction amount was calculated between the output and hidden layers, even between the hidden layers and the input layers. The iterative cycle moves back and forth till the achievement of an optimal error between the network output and the intended output (Faisal et al. 2021; Gopal and Woodcock 1996; Maduako et al. 2016a, b; Mansour et al. 2020). Detailed methodology is shown in Fig. 5.

Five hidden layers, i.e., classified LULC images, NDBI, NDBSI, latitude, longitude, were considered input parameters and the extracted LST data were considered output parameters for LST prediction. Hidden layers are essential for the prediction method as these influence the outcome allowing the network to manifest non-linear behavior. The initial rate (μ) was set at 0.1, and the range of decay (β) that ranges between 0 and 1 was used to monitor it (Shatnawi and Abu Qdais 2019; Van Gerven and Bohte 2017). The pixel value data were converted to discrete data for all the images to better the performance of the ANN model. The prediction process consists of network development, assessment of network performance, network training, and prediction. For accuracy assessment of the intended data in representing the changes in the

performance tests, a regression analysis was done (Arsanjani et al. 2013; Hu and Lo 2007), which provided the Mean Square Error (MSE) and Coefficient Correlation (R) values that determined the network confidence (Faisal et al. 2021; Maduako et al. 2016a, b; Nurwanda and Honjo 2020; Ullah et al. 2019b). To validate the model, R and MSE values of 2020 for the summer and winter seasons were obtained.

Result and discussion

This section describes the results estimated from the methodology mentioned in the “Data and methodology” section. The results contain a spatiotemporal change of LULC, variation of seasonal LST, seasonal LST distribution over different LULC classes, prediction of the future LULC classes, and seasonal LST distribution. This section finally discusses FGDs and KIIs findings and proposes effective strategies for ensuring sustainable land use management, reduction in temperature increase, and possible mitigating measures to combat climate change impacts.

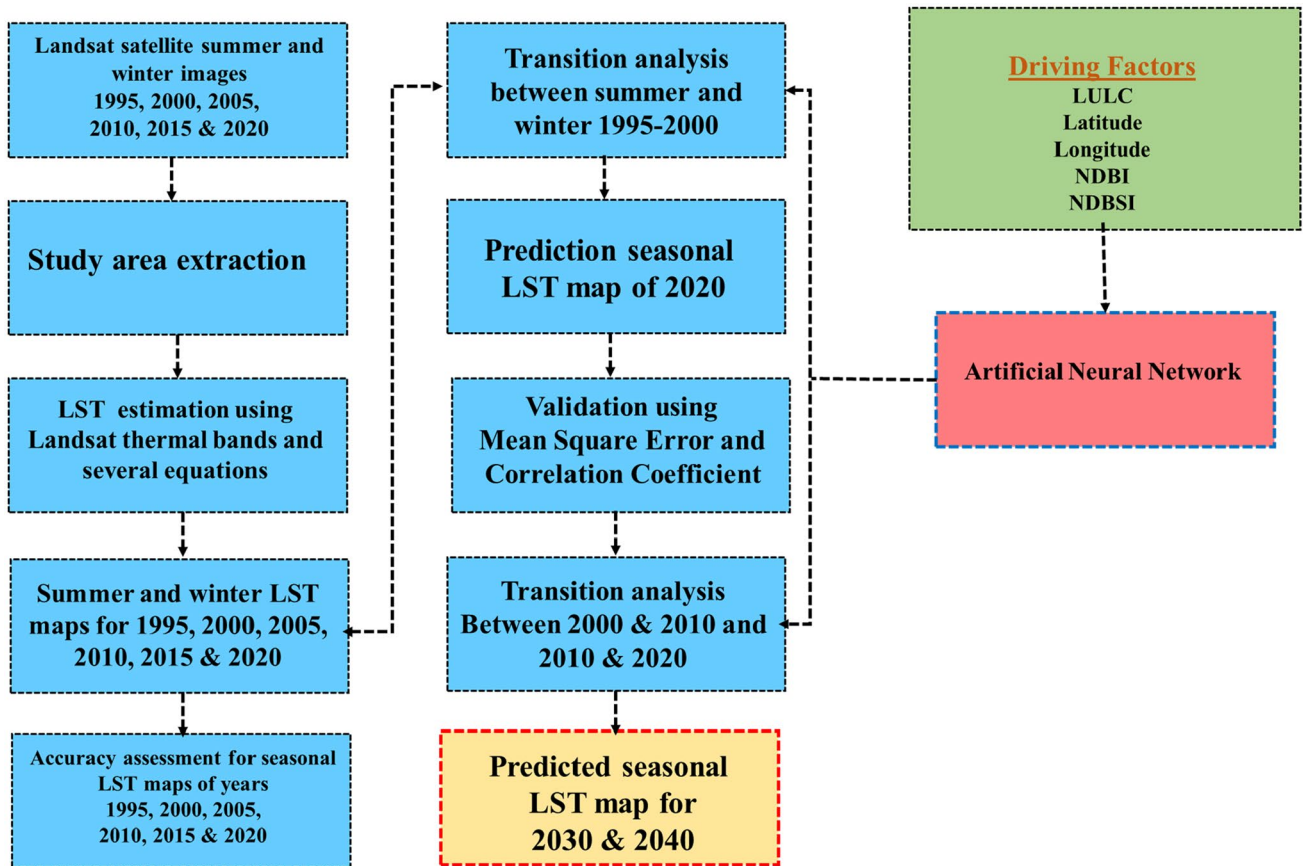


Fig. 5 Flowchart of seasonal LST prediction process using ANN algorithm

Spatiotemporal change of LULC (1995–2020)

The spatiotemporal distribution of classified LULCs, i.e., water bodies, built-up area, agricultural land, and bare land for 1995, 2000, 2005, 2010, 2015, and 2020 are illustrated in Fig. 6. The accuracy assessment of the classified maps shows a higher accuracy with more than 89% overall accuracy for all the years (Table 4), which is considered an excellent accuracy percentage for further analysis (Wang et al. 2017).

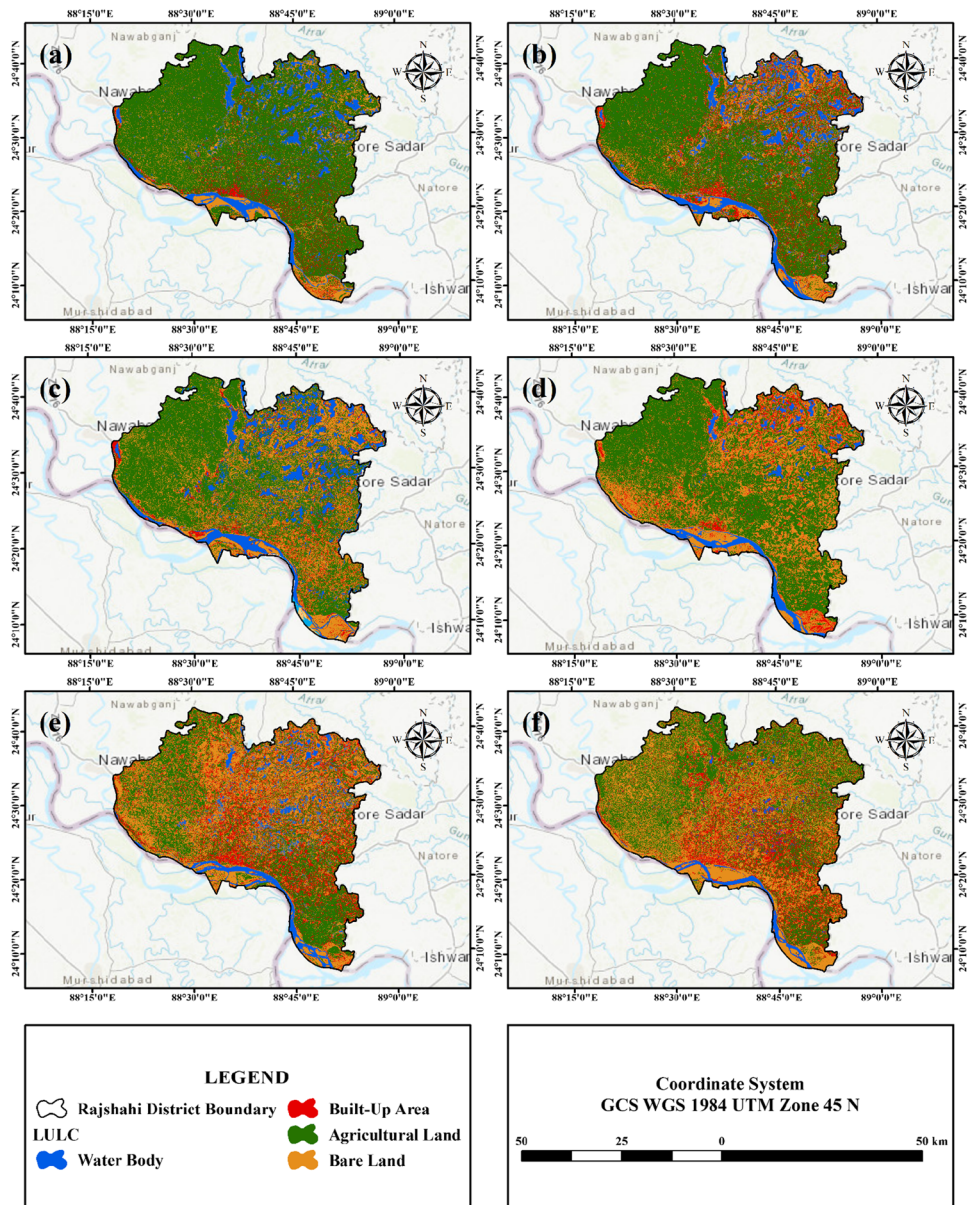
The areal distribution of LULC during 1995–2020 is shown in Fig. 7. Two changing trends are noticed from the areal analysis. One is a massive decrease of agricultural lands and a gradual increase of built-up areas. The agricultural land was 1461.92 km² (61.37%), 1281.12 km², and 1209.86 km² by 1995, 2000, and 2005 respectively, showing a massive decrease in 2010 (1194.04 km²) and 2015 (1005.39 km²), ultimately resulting in a 926.14 km² (38.88%) of agricultural land in 2020. On the other hand, the built-up area consisted only 158.22 km² (6.64%), 167.53 km², and 195.27 km² of the total land in 1995, 2000, and 2005 that was experienced a steady increase in 2010 (225.23 km²) and 2015 (300 km²), finally reached to an area

of 386.74 km² (16.23%) in 2020. Significant changes were also noticed for water bodies and bare land classes. In 2020, 7.54% and 37.37% water bodies and bare land classes were estimated, which were 14.17% and 17.82% in 1995.

A detailed temporal change of the LULC classes pattern is shown in Table 5. A steady increase during 1995–2000 (0.39%), 2000–2005 (1.16%), and 2005–2010 (1.26%) was noticed in built-up area followed by a massive increase in 2010–2015 (3.14%) and in 2015–2020 (3.64%). Another upsurge scenario was estimated in bare land as the major increase occurred during 1995–2000 (9.28%) and 2010–2015 (5.27%). A major decrease was recorded in agricultural land during 1995–2000 (–7.59%) and 2010–2015 (–7.92%), same timelines as major increases were estimated for bare lands. A gradual decrease in agricultural land was seen during 2000–2005 (–2.99%) and 2015–2020 (–3.33%). Waterbody has experienced a major decrease until 2010, as analysis showed by 2.08%, 1.4%, and 2.27% decrease rate during 1995–2000, 2000–2005, and 2005–2010 timeline, respectively.

The analysis shows a significant uncontrolled growth in built-up areas and a remarkable decrease in agricultural lands and water bodies. Rapid haphazard urban planning

Fig. 6 Classified LULC images of Rajshahi district for **a** 1995, **b** 2000, **c** 2005, **d** 2010, **e** 2015, and **f** 2020



and uncontrolled rural–urban migration due to the pull factors (better job opportunities, the standard of livings, better healthcare facilities, etc.) are some of the main reasons behind this significant LULC change. The cool land covers like agricultural lands and water bodies are constantly filled with impervious surfaces of built-up area to cover the increasing infrastructure demand by rapidly grown housing projects. Reduced agricultural areas result in a rise in uncontrolled and intensive agriculture, which increases the use of chemical elements and pesticides, resulting in harm to the environment’s most vital elements, namely water, air, and soil (Faisal et al. 2021; Wang et al. 2017). Also, a significant reduction of green cover will reduce the functions of biodiversity and ecosystem services. Due to the surface water body losses, pressure will increase in groundwater,

which will create water scarcity during agricultural production in upcoming years.

Variation of seasonal LST distribution in the study area

Landsat thermal bands were used to extract the seasonal variation (both summer and winter) of LST in the study region during 1995–2020. Summer and winter maximum and minimum LST distribution are illustrated in Fig. 8 and Fig. 9, respectively.

Summer LST distribution shows a maximum temperature of 37.22 °C and 38.4 °C in 1995 and 2000 respectively that gradually was increased to 38.83 °C in 2005 and 39.72 °C in 2010, resulting in more increased in maximum temperature

Table 4 Accuracy assessment of the classified images

Year	Classified class	Validation points for different LULC classes					User accuracy
		Water body	Urban area	Vegetation cover	Bare land	Total	
1995	Water body	61	1	2	1	65	93.85
	Urban area	0	84	1	4	89	94.38
	Vegetation cover	1	4	58	9	72	80.56
	Bare land	1	5	3	65	74	87.84
	Total	63	94	64	79	300	
	Producer accuracy	96.83	89.36	90.63	82.28	Overall accuracy 89%	Kappa coefficient 85.69
2000	Water body	59	2	1	1	63	93.65
	Urban area	0	83	3	4	90	92.22
	Vegetation cover	1	2	71	3	77	92.21
	Bare land	0	5	3	62	70	88.57
	Total	60	92	78	70	300	
	Producer accuracy	98.33	90.22	91.03	88.57	Overall accuracy 92%	Kappa coefficient 88.81
2005	Water body	64	1	0	0	65	98.46
	Urban area	2	81	2	1	86	94.19
	Vegetation cover	1	3	69	3	76	90.79
	Bare land	0	1	2	70	73	95.89
	Total	67	86	73	74	300	
	Producer accuracy	95.52	94.19	94.52	94.59	Overall accuracy 94%	Kappa coefficient 92.87
2010	Water body	53	2	4	2	61	86.89
	Urban area	0	78	2	4	84	92.86
	Vegetation cover	1	3	77	3	84	91.67
	Bare land	2	4	3	62	71	87.32
	Total	56	87	86	71	300	
	Producer Accuracy	94.64	89.66	89.53	87.32	Overall accuracy 90%	Kappa coefficient 89.22
2015	Water body	51	1	2	2	56	91.07
	Urban area	1	81	4	4	90	90.00
	Vegetation cover	1	3	71	3	78	91.03
	Bare land	2	4	5	65	76	85.53
	Total	55	89	82	74	300	
	Producer accuracy	92.73	91.01	86.59	87.84	Overall accuracy 89%	Kappa coefficient 85.65
2020	Water body	55	2	1	1	59	93.22
	Urban area	0	80	2	4	86	93.02
	Vegetation cover	1	3	70	3	77	90.91
	Bare land	1	4	5	68	78	87.18
	Total	57	89	78	76	300	
	Producer accuracy	96.49	89.89	89.74	89.47	Overall accuracy 91%	Kappa coefficient 87.92

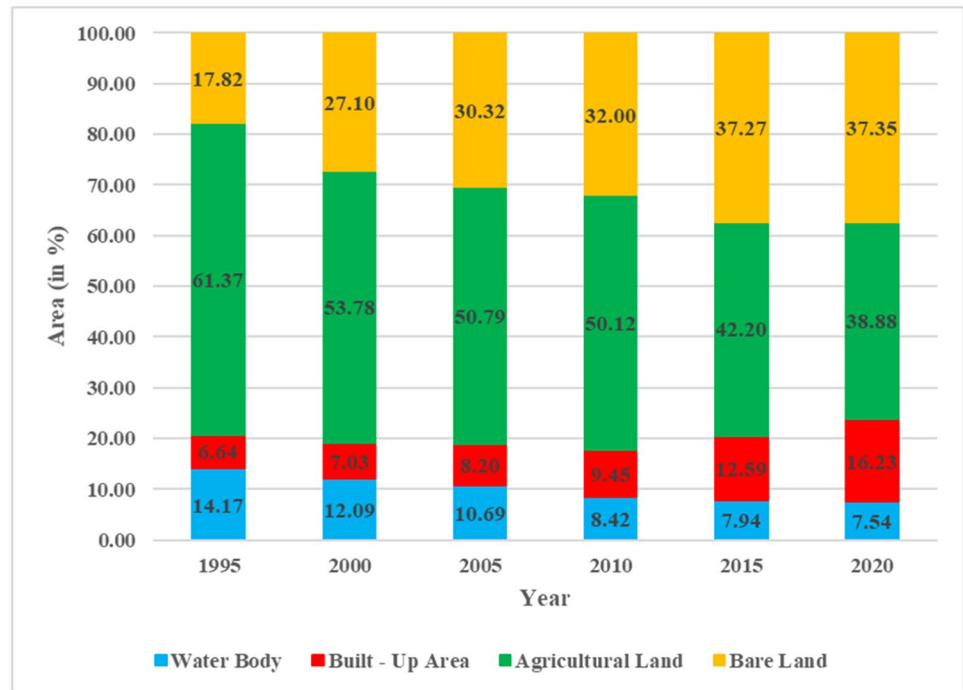
in 2015 (41.36 °C) and 2020 (42.7 °C) by creating a deviation of approximately 1 °C for every 5 years. The same increasing pattern was seen in minimum temperature too as the minimum temperature in 1995, 2000, 2005, and 2010 was 22.18 °C, 23.32 °C, 24.68 °C, and 26.31 °C respectively with a deviation of 2 °C on an average, leading to a minimum temperature of 27.52 °C in 2015 and 28.94 °C in 2020.

Winter LST distribution also shows a steady increasing pattern as the maximum temperature in 1995, 2000, 2005, and 2010 were 24.53 °C, 25.82 °C, 26.34 °C, and 27.34 °C showing a gradual increasing rate with an average deviation

of approximately 1 °C, resulting in a maximum temperature of 28.54 °C in 2015 and 29.12 °C in 2020. A similar increase rate was also seen in the minimum temperature of the winter season as in 1995, 2000, 2005, and 2010 the minimum temperature were 14.67 °C, 15.11 °C, 16.27 °C, and 17.52 °C respectively that steadily increased to 18.91 °C and 20.42 °C in 2015 and 2020 respectively with 1 °C average deviation between 5 years.

Both summer and winter LST distribution in the study area shows an increasing trend in the south, south-east, north-east, and northern part of the study area. However, the

Fig. 7 Areal distribution of different LULC during the study period (1995–2020)



western part of the study area did not experience the same increasing pattern as the eastern part due to the massive LULC change in the eastern and southeastern parts (Fig. 6). Climate change, global warming, unplanned urbanization, increase in the impervious layers (buildings, roads, and

highways), greenery, and water bodies reduction in the study region may be responsible for this seasonal increase in LST (Alamgir et al. 2020; IPCC 2014). The significant increase in LST reduces the accessibility of water and crops, thereby increasing the vulnerability to drought and extreme weather conditions in the study region. Due to massive climate changes and global warming, winter in the study region is gradually warmer (Bank 2016; IPCC 2014). Climate change experts and meteorologists predicted that the winter season would be significantly warmer and shorter than in previous years, as the temperature continues to rise daily.

Table 5 Spatiotemporal change of different LULC during the different time periods

Time range	Net change in %			
	Water body	Built-up area	Agricultural land	Bare land
1995–2000	-2.08	0.39	-7.59	9.28
2000–2005	-1.40	1.16	-2.99	3.22
2005–2010	-2.27	1.26	-0.66	1.67
2010–2015	-0.49	3.14	-7.92	5.27
2015–2020	-0.39	3.64	-3.33	0.08
1995–2005	-3.48	1.56	-10.58	12.51
1995–2010	-5.75	2.81	-11.25	14.18
1995–2015	-6.24	5.95	-19.16	19.45
1995–2020	-6.63	9.59	-22.49	19.53
2000–2010	-3.67	2.42	-3.66	4.90
2000–2015	-4.15	5.56	-11.57	10.17
2000–2020	-4.55	9.20	-14.90	10.25
2005–2015	-2.76	4.40	-8.58	6.94
2005–2020	-3.15	8.04	-11.91	7.02
2010–2020	-0.88	6.78	-11.25	5.35
	Overall change in %			
1995–2020	-3.19	4.39	-9.86	8.65

Spatial distribution of seasonal LST on different LULC

To evaluate the seasonal mean LST distribution in different classified LULCs, i.e., waterbodies, built-up area, agricultural land, and bare land, the “zonal statistics” tool was used in ArcGIS 10.6 software. Figure 10 represents the mean seasonal temperature fluctuation in various LULC classes during the study period (1995–2020) with a 5-year interval.

A significant increase in the summer LST variation in different LULC, especially in a built-up area and bare land, was recorded in the spatial distribution. Summer mean LST in built-up areas were increased from 37.26 °C (2010) to 41.68 °C in 2020, which was 34.92 °C in 1995. In bare land, summer mean temperature was 32.77 °C in 1995 that was increased to 36.12 °C in 2015 and 38.06 °C in 2020. Deviation of 6.76 °C and 5.29 °C was seen in summer mean temperature of built-up areas and bare land, during

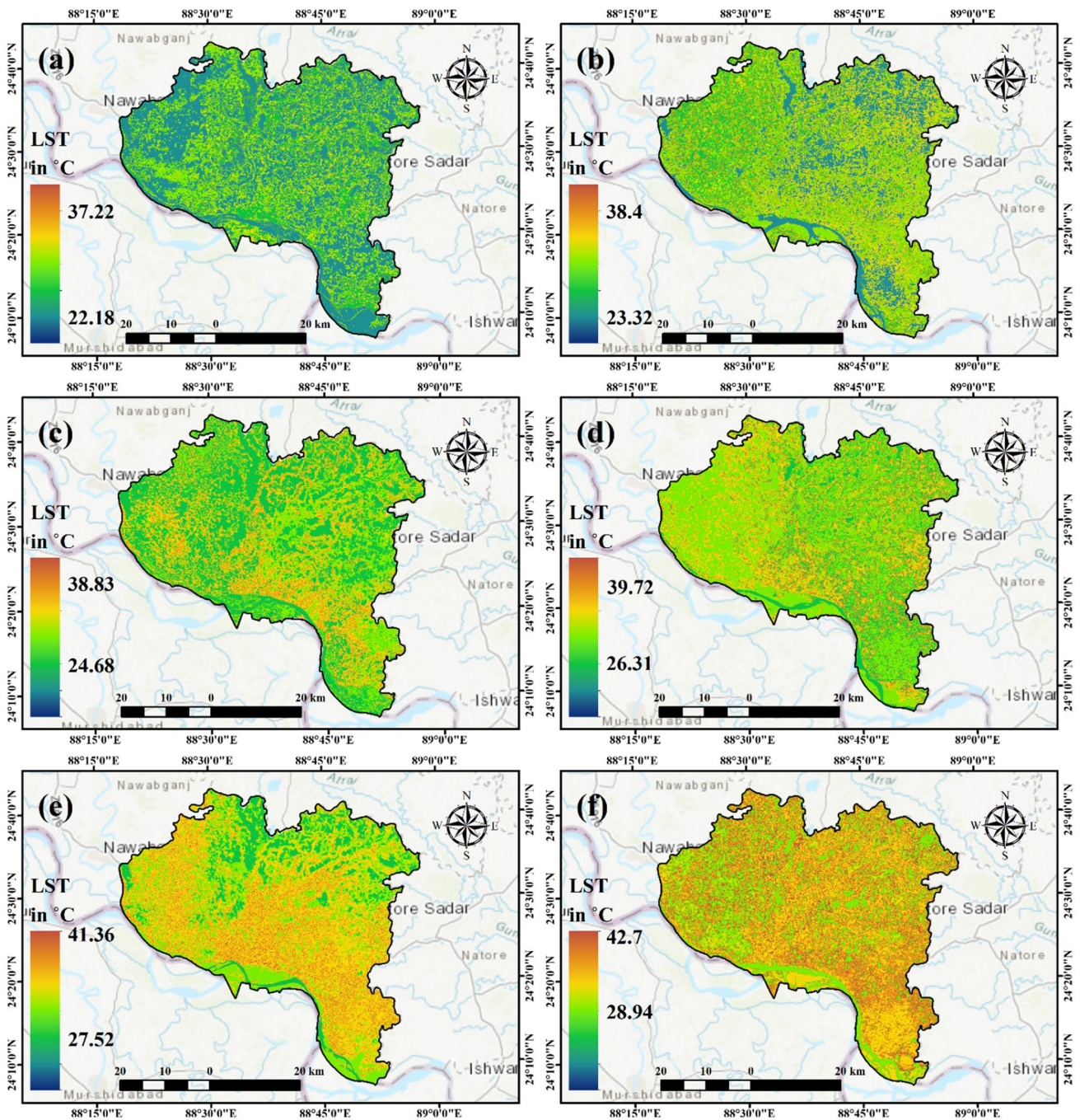


Fig. 8 Spatial distribution of summer LST of the study area in **a** 1995, **b** 2000, **c** 2005, **d** 2010, **e** 2015, and **f** 2020

the study period (1995–2020). The distribution of LST in agricultural land and water bodies was also changed as in agricultural land, the mean summer temperature in 1995 was 25.31 °C that was increased to 31.02 °C in 2015 and 31.72 °C in 2020, having a deviation of 6.41 °C during the study period (1995–2020). The mean summer LST in water bodies was 24.46 °C in 1995, the lowest

mean temperature was recorded in summer, followed by an increment to 28.37 °C in 2015 and 29.88 °C in 2020.

Variation of winter mean LST had also shown a significant increase in different LULC. Winter mean LST in built-up areas was 22.35 °C in 1995 followed by 26.88 °C and 28.35 °C in 2015 and 2020, respectively, having an escalation of 6 °C during the study period (1995–2020). In bare

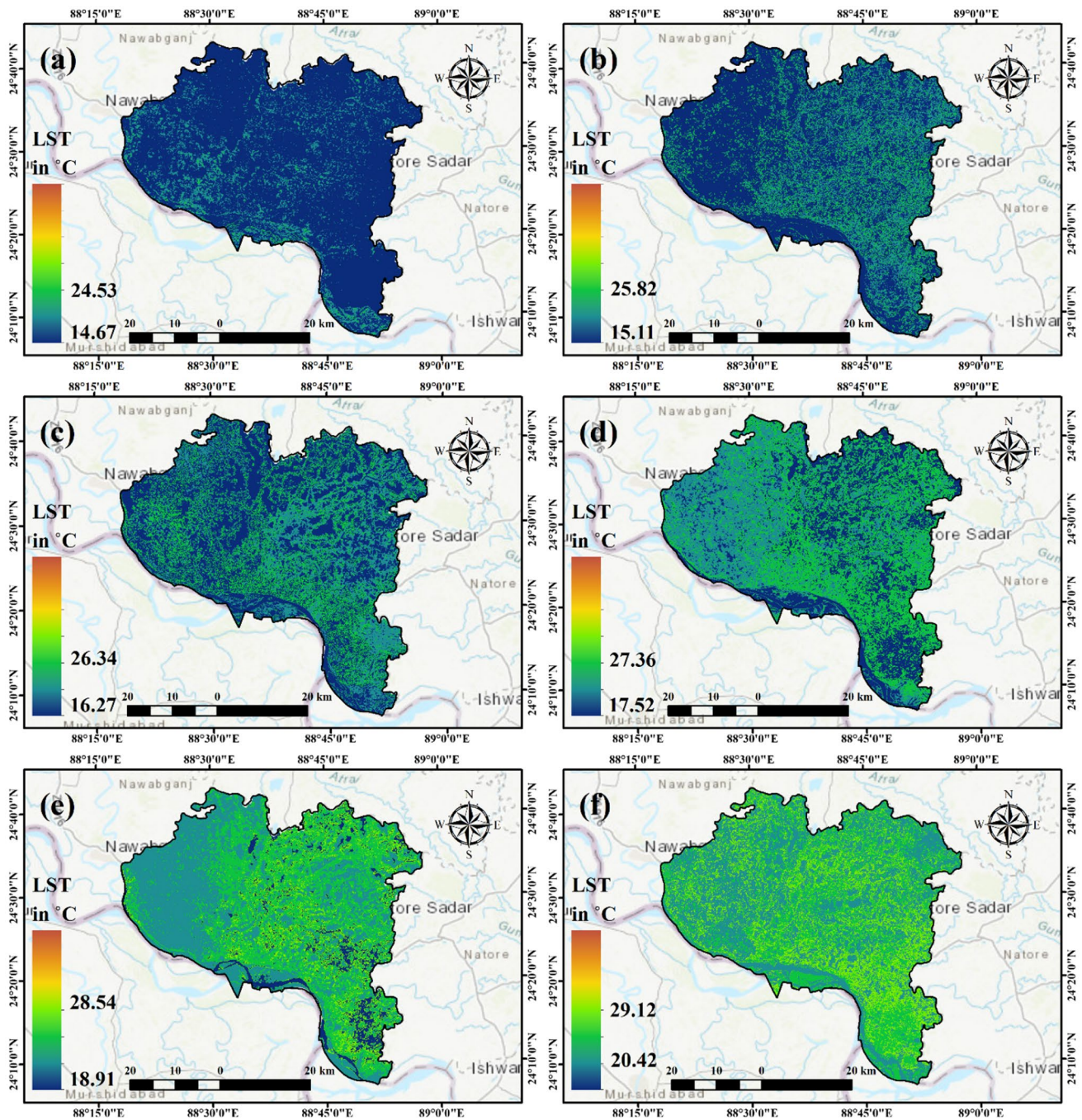


Fig. 9 Spatial distribution of winter LST of the study area in **a** 1995, **b** 2000, **c** 2005, **d** 2010, **e** 2015, and **f** 2020

lands, the winter mean temperature in 1995 was 21.76 °C, which was increased to 25.65 °C in 2015 and 26.39 °C in 2020 with a deviation of 4.63 °C from 1995 to 2020. Water bodies and agricultural lands also experienced a gradual increase in the winter mean temperature. In agricultural lands, the mean winter temperature in 1995 was 15.38 °C, followed by an enlarged temperature of 20.33 °C in 2015 and 21.74 °C in 2020. The mean winter LST of the water body

was also increased to 19.32 °C in 2015 and 20.87 °C in 2020 from the low temperature of 14.92 °C in 1995. An increase of 5.95 °C and 6.36 °C was recorded in the winter mean temperature of water bodies and agricultural lands, respectively, during the study period (1995–2020). The highest winter mean temperature was recorded in the built-up area for 2020 (28.35 °C), and the lowest winter mean temperature was recorded in the water body for 1995 (14.92 °C).

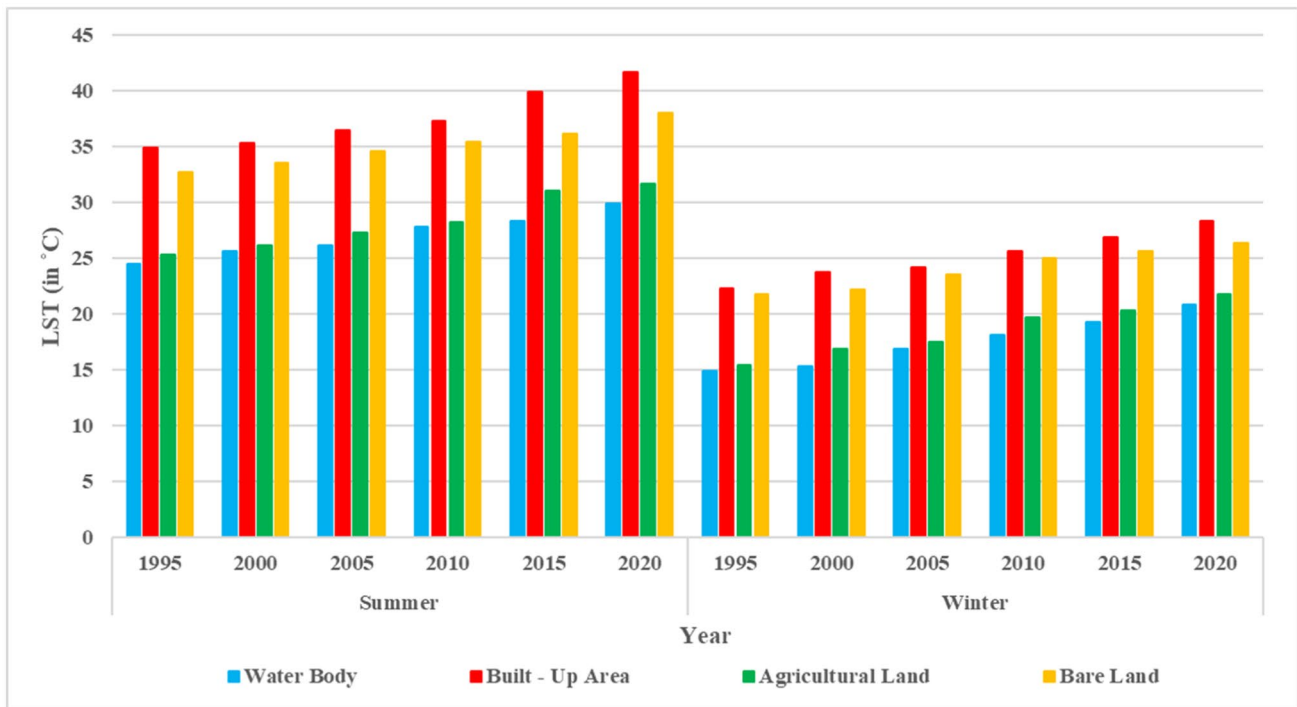


Fig. 10 Mean LST distribution in different LULC during the study period (1995–2020)

The variation of seasonal mean LST on different LULC shows an analytical insight about the adverse effect of built-up area in the gradual increment of LST by replacing the cool LULC classes (agricultural lands and water bodies) with the impervious surfaces (built-up areas). Uncontrolled and rapid urban development, rural to urban migration, climate change, and global warming are few of the most significant contributors to the temperature rise. Green covers of agricultural and vegetation lands have penetrable layers and tree shading that can help in less heat emission to reduce the heat (Djekic et al. 2018). However, with the unplanned development, these green covers are constantly replaced with the major portion of impervious and paved surfaces that can retain more energy and radiate more heat thus increasing the temperature (Al Rakib et al. 2020a; Fahad et al. 2018; Rahman et al. 2017a, b).

Predicted scenario of future LULC dynamics

The future prediction scenarios for LULC classes for 2030 and 2040 were performed using the CA algorithm (Fig. 11). Classified LULC maps for the years 2000 and 2010 were used to predict the 2030 scenario, where 2010 and 2020 maps were used to predict the 2040 LULC scenario. For evaluating the accuracy of the prediction model, a predicted map for 2020 was done using the past LULC maps (2000, 2010, and 2015). The QGIS and TerrSet

were used to validate the CA model, and both techniques presented an excellent prediction accuracy for the future LULC scenario. The QGIS validation shows more than 88% correctness and 0.8 Kappa value for the predicted image (Table 6). Kappa parameters evaluation in TerrSet shows satisfactory results as $K_{location}$, K_{no} , $K_{location\ strata}$, $K_{standard}$ values showed more than 0.8 for the predicted image. Therefore, the estimated kappa and the percentage (%) of correctness value were satisfactory and suitable to predict the future LULC scenario for 2030 and 2040 (Pontius and Millones 2011).

Comparing the predicted maps of 2030 and 2040 with the classified scenario of 2020 shows that 59.8 km² area in 2030 and 126.09 km² area in 2040 will face infrastructural development if proper measures are not taken. Due to rapid built-up area expansion, agricultural land (– 2.41% in 2030 and – 6.22% in 2040) and water body (– 0.98% in 2030 and – 2.77% in 2040) will face a significant decrease in the predicted years. The highest positive net change was recorded for built-up areas (2.51% and 5.29%), where the maximum negative net change was noticed for agricultural land (– 2.41% and – 6.22%) from 2020 to 2030 and 2020 to 2040, respectively (Table 7). The expected LULC shift demonstrated that if not properly controlled, the increasing rate of built-up areas could have a severe impact on future ecosystem services, environmental sustainability, and human life.

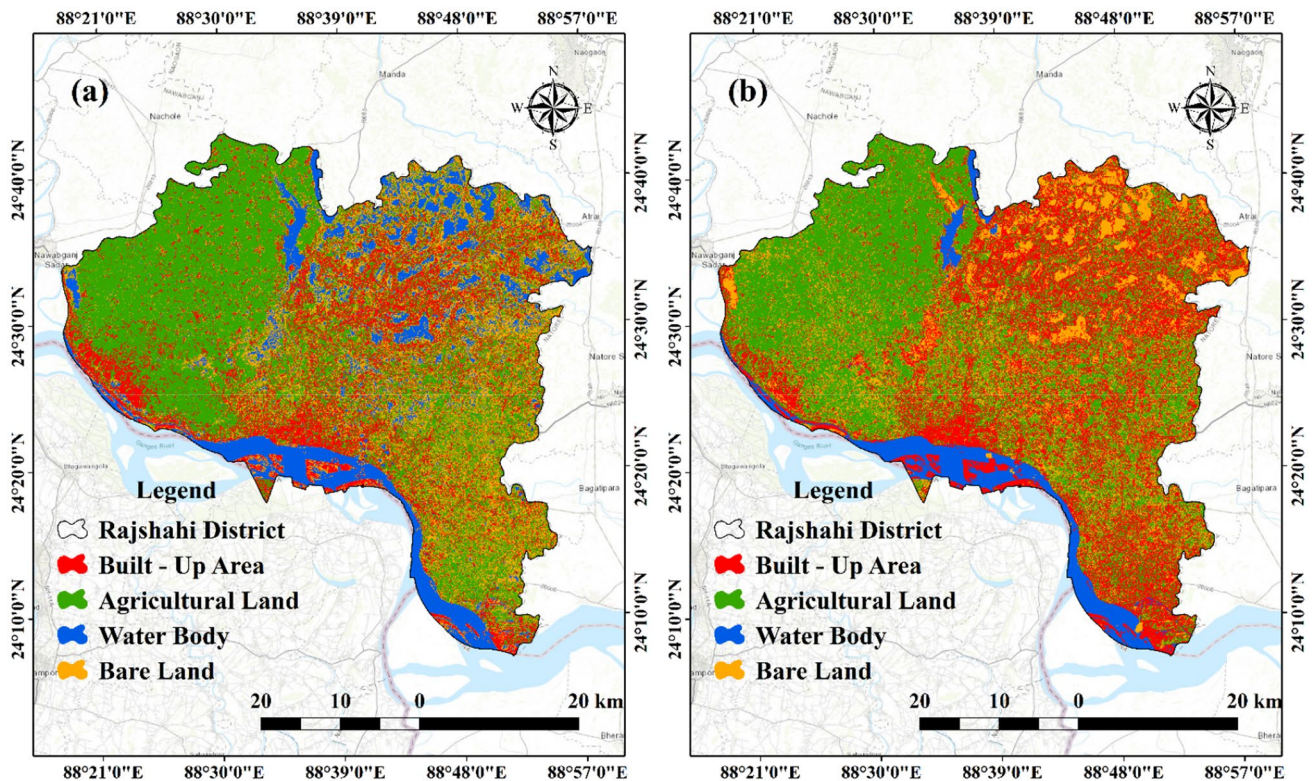


Fig. 11 Predicted future LULC maps for a 2030 and b 2040 in the study area

Table 6 CA model accuracy validation using QGIS and TerrSet for the predicted maps of 2020

Prediction year	CA model validation with two platforms					
	Kappa parameters of TerrSet				QGIS MOLUSCE Plugin Model	
	$K_{location}$	K_{no}	$K_{location\ strata}$	$K_{standard}$	%—correctness	Overall Kappa value
2020	0.82	0.85	0.80	0.82	88.35	0.82

Table 7 Predicted LULC scenario of 2030 and 2040 with a comparison of 2020 LULC scenario

LULC classes	Area (in km ²)			Net change (in %)			Overall change (in %)
	2020	2030	2040	2020–2030	2030–2040	2020–2040	
Water body	179.66	156.28	113.68	-0.98	-1.79	-2.77	-1.85
Built-up area	386.74	446.54	512.83	2.51	2.78	5.29	3.53
Agricultural land	926.14	868.62	777.95	-2.41	-3.81	-6.22	-4.15
Bare land	889.68	910.78	977.76	0.89	2.81	3.70	2.47

Predicted seasonal distribution of LST

The seasonal LST variation during the study period (1995–2020) showed a significant escalation in the temperature. Thus, it is critical to predict future seasonal LST distribution dynamics to understand the potential threat to environmental sustainability and climate change in the study area. The ANN algorithm was used to predict the future

seasonal LST scenario for 2030 and 2040 using the past LST trends (2000–2010 and 2010–2020), and the predicted summer and winter LST are illustrated in Fig. 12 (a and b) and Fig. 13 (a and b), respectively. The comparison of the predicted seasonal LST scenario of 2020 with the actual estimated LST of the same year showed a promising agreement proving the model’s accuracy and validation. The MSE values for both seasons were less than 0.6 for the LST

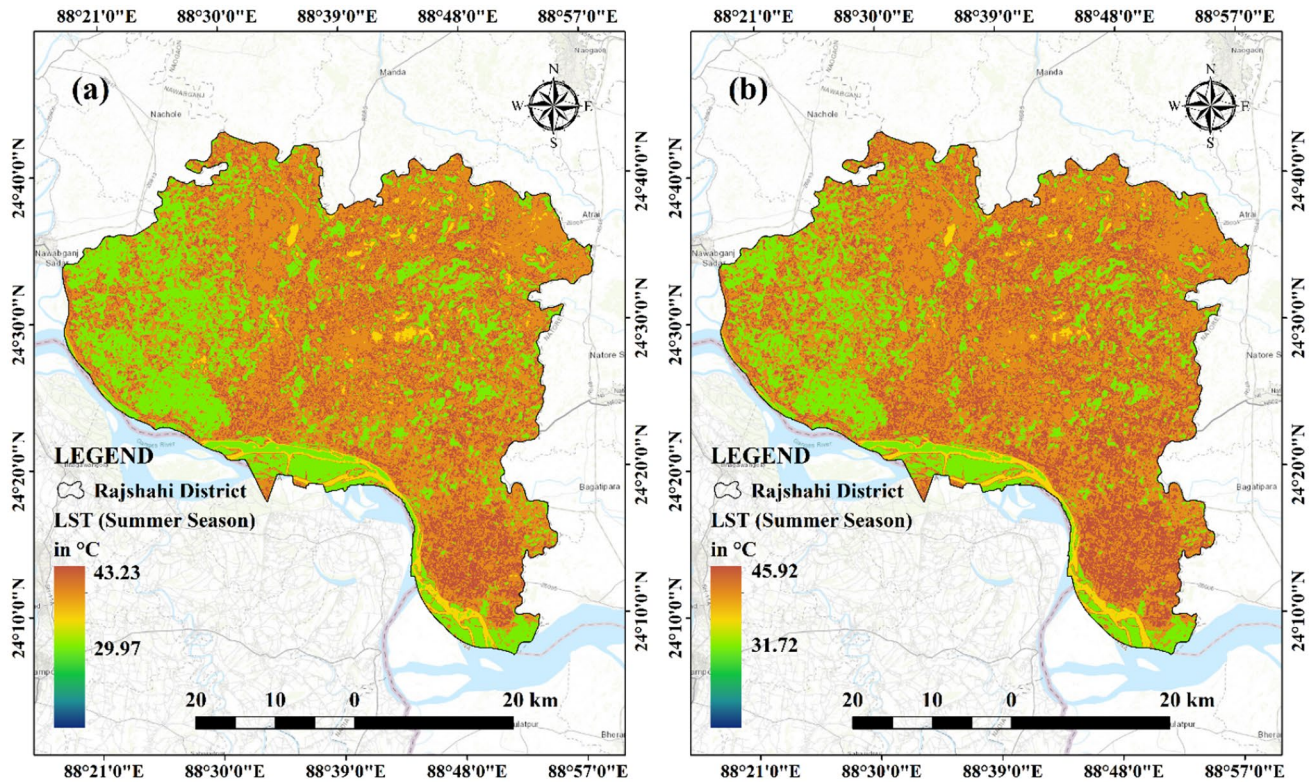


Fig. 12 Predicted summer LST Scenario of a 2030 and b 2040

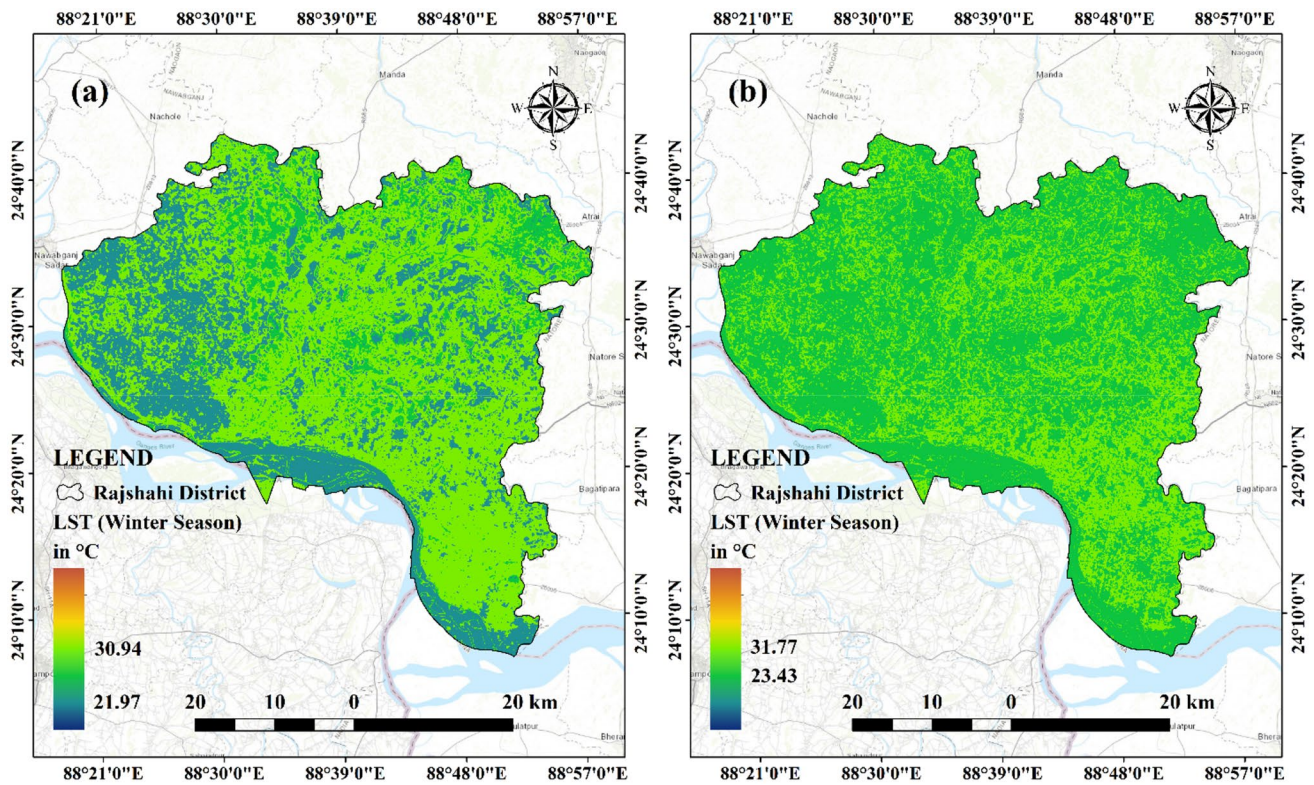


Fig. 13 Predicted winter LST Scenario of a 2030 and b 2040

scenario, and the R values were greater than 0.8, showing a strong positive correlation with the estimated and predicted LST (Table 8).

Figures 10 and 11 show a similar increasing trend in the seasonal temperature over the study area in 2030 and 2040. The Summer LST trend shows the maximum temperature will likely be increased to 43.23 °C in 2030 and 45.92 °C in 2040 from 42.7 °C in 2020. The minimum summer temperature of 2030 and 2040 will be increased to 29.97 °C in 2030 and 31.72 °C in 2040 from 28.94 °C in 2020, having an approximate increase of 1 °C between 2020 and 2030 and 3 °C between 2020 and 2040.

Winter LST trend shows a similar increasing scenario in 2030 and 2040. In 2030, the maximum winter temperature will be expected to be reached at 30.94 °C (2030) and 31.77 °C (2040), where the minimum winter temperature in 2030 and 2040 will be 21.97 °C and 23.43 °C, respectively. Compared to the 2020 winter LST distribution, the maximum and minimum temperature average increment rate for 2030 and 2040 were 1.7 °C and 2.8 °C, respectively.

This increasing seasonal LST trend affects the thermal capacity of different LULC categories and contributes to the UHI effect (Bonafoni et al. 2017). Moreover, according to the fifth IPCC assessment report, Asian regions are expected to hit higher temperatures than the global average (IPCC 2014). Intensification to urban areas compared to rural areas greatly influences the uplifting of global warming (Roy et al. 2014). An increase in the green cover through preservation of the agricultural land, afforestation, planned urban planning approach, and employment of urban planners in government authorized city planning organizations can help to control the unplanned urbanization and uncontrolled temperature rise and can able to mitigate the UHI effect (Faisal et al. 2021).

Limitations of CA and ANN models

The CA and ANN models showed excellent performances in predicting the LULC and LST change dynamics for 2030 and 2040 using the previous datasets during the study period. However, the CA and ANN models provide an

efficient framework for analyzing and forecasting LULC and LST scenarios. The models are more accurate when the historical pattern of LULC and LST dynamics remains constant or fixed. As a result, the CA model is not always adequate for explicitly predicting spatial LULC (Santé et al. 2010). Because of its limited ability to identify the explicit relationship between the influential variables, the ANN is sometimes referred to as a black box (Van Gerven and Bohte 2017). The ANN model develops training samples following the input of layers and begins to train and determine the most influential variables without considering their relative significance. There are no well-established criteria in the system for weighting each input parameter individually according to its significance (Shatnawi and Abu Qdais 2019). However, dynamic phenomena such as urbanization, loss of green cover, and surface temperature rise cannot be anticipated with 100% precision since they are heavily dependent on human activities and rational decisions made at the regional to the municipal level.

Whatever their limits, dynamic models are helpful for assumptions and understanding the phenomenon of changes in the land cover and variations in surface temperature in any area. Techniques such as LULC, LST change, and prediction mapping are rapidly gaining recognition as highly effective tools for managing critical natural resources and mitigating environmental consequences.

Impact on LULC, seasonal LST, and climate change based on KIIs and FGDs

This section briefly describes the outcomes of FGDs and KII. The FGDs outcome will help to understand the impacts of LULC and temperature changes on the study area in the last 25 years. Along with the KIIs assessments, experts' opinions will assist in identifying the possible impacts of climate change on the study region.

Group discussion related impacts of LULC change and temperature increase

During the FGDs, participants were asked questions about the effects of LULC changes in the research area over the last 25 years (1995–2020). The key investigation points in the FGDs were questions about the impact of LULC on temperature, agricultural land, biodiversity, soil characteristics, and water resources. During the ten focus groups, a total of 76 people took part. The participants were given a sheet that included all of the potential LULC effects stated in the table and allowed them to select various options ranging from very low to very high for all of the questions. According to the findings of the discussion, massive LULC change significantly increases seasonal temperature (71% very high),

Table 8 ANN Model validation with the predicted and observed seasonal LST of 2020

Prediction year	Season	ANN model validation for LST prediction using MATLAB software		
		No. of hidden layers	Mean Square Error (MSE)	Correlation Coefficient (R)
2020	Summer	5	0.52	0.86
	Winter		0.59	0.84

converts agricultural land and other green cover areas into infrastructure (69% very high), disrupts the hydrological cycle by increasing groundwater stress and reducing surface water bodies (51% very high), and ultimately causes flooding. Furthermore, LULC has a large impact on biodiversity and habitat destruction (65% high) by converting agricultural and green cover areas to infrastructure (Table 9). The results of the FGDs will also validate the results obtained from satellite image observation, which show that significant LULC change is occurring in the study area, particularly agricultural land being converted to built-up areas and that the overall seasonal LST is increasing due to the increase in impervious layers.

Interviewed related impacts on climate change in the study region

During the KIIs, experts were asked questions on the effects of climate change in the study area. During the KIIs, questions about the impact of climate change on seasonal variations, heat and cold waves, decrease in rainfall, agricultural production, change in irrigation source, time of sowing seeds, and so on were asked. The total number of KII participants was 20, and during the interview, possible climate change impacts were presented to the experts on a sheet, allowing them to select multiple options as well as any other impact based on their expertise. According to the findings of the KIIs, climate change has significantly increased heat waves (76% very high) and impacted seasonal variations (66% very high), resulting in a longer summer and a significantly shorter winter season. Furthermore, climate change alters the rainfall pattern, increasing the pressure on the surface and groundwater (very high 64%). Experts also suggested that increased use of fertilizer, insecticides, and changes in seeding time reduce agricultural and fish productivity (very high 88%) (very high 62%). Due to climate change, original species of paddy and fish are becoming extinct and being replaced by artificial/bred species of fish. As a result, many people are malnourished. According to experts, agriculture is one of the most vulnerable sectors to

climate change, as it is primarily influenced by temperature changes, rainfall patterns, and the increased likelihood of extreme events (drought and floods). According to experts, climate change hastens the occurrence of climate-sensitive diseases (high 60%), such as hypertension associated with heat stress, diarrhea, dengue, dysentery, and so on. Experts also stated that the urban poor are particularly vulnerable to the effects of climate change (up to 60%) due to the infrastructural fragility of slums and squatter settlements and a lack of job security. The results of the KIIs will also support the findings of the satellite image analysis, which show that climate change and the loss of green cover by built-up areas significantly contribute to summer and winter seasonal variations, long summer and winter season time duration, and a reduction in ecosystem and biodiversity (Table 10).

Sustainable land use management, temperature increase, and climate change mitigating strategies

Based on the suggestions provided by the FGD and KII participants, strategies for ensuring sustainable land use management, reducing the upsurge of temperature, and mitigate the climate change impacts have been developed. The implementation of these strategies will ensure planned sustainable infrastructural development by ensuring integrated local–regional intergovernmental coordination between different organizations.

- i. Ensuring proper use of available land by restricting the unplanned expansion of infrastructural development and conserving natural resources like green covers and water bodies.
- ii. Promoting vertical infrastructural development, restricting the misuse of bare lands, and utilizing available open land for activities related to nature-based solutions like tree plantation and water resource management.
- iii. Applying zoning techniques at the regional-local level to identify the locations of natural resources and

Table 9 Group discussion outcomes of possible impacts of LULC change in the study area

Impact of LULC change	Changes in last 25 years (in %); N=76				
	Very low	Low	Moderate	High	Very high
Increase in seasonal temperature	7	5	17	35	71
Agriculture lands and green cover converted to infrastructure	2	3	23	41	69
Reduction of agricultural land (green area) contributes to biodiversity loss and destroys habitats	0	4	12	65	21
The rapid transformation of the green area increases soil erosion, desertification due to intensive cultivation in the same land	0	1	11	19	49
LULC changes disturb the hydrological cycle, reduce surface water bodies and create flooding by increasing surface runoff	2	4	16	45	51

Table 10 Outcomes of expert interviews related to possible impacts of climate change in the study area

Possible climate change impacts	<i>N</i> =20 (in %)				
	Very less	Less	Moderate	Much	Very much
Impact on agriculture (decrease crops production and quality) and fisheries	0	0	21	51	88
Reduces biodiversity	0	0	28	41	58
Increase stress on water resources and hydrology	0	0	35	47	64
Increased moisture stress during dry periods leading to increased drought	1	1	11	24	57
Greater temperature extremes	0	0	38	59	76
Impact on seasonal variations	0	0	21	29	66
Changes in precipitation patterns	2	3	13	33	29
Increase in crops growing season	4	6	26	59	62
Increased vulnerability to cyclone and storm surges	3	5	51	9	21
Impacted on human health	0	2	26	60	33
Particularly more impact on vulnerable groups like urban poor	0	5	16	57	25

ensure infrastructural development by conserving them.

- iv. Safeguarding the gradually declining trend of agricultural lands by imposing strict rules and regulations to feed the growing population, enhance economic enlargement, and preserve biodiversity.
- v. Increasing more artificial wetlands and introduce rain-water harvesting approach for reducing pressure on groundwater and adequate recharge of the aquifer.
- vi. Applying integrated water resource management (IWRM) plan for ensuring sustainable use of surface and groundwater resources.
- vii. Preventing water, soil pollution and increase the surface water availability for higher agricultural productivity and environmentally sustainable land utilization.
- viii. Increasing green landscape around households by tree plantation and rooftop farming to combat heat waves, which will improve air quality, and reduce heat stress-related health problems.
- ix. Ensuring sustainable infrastructural development by preparing an integrated local–regional level master plan with the help of urban planners for planned and inclusive urbanization by conserving natural resources.
- x. Proper coordination between local and regional level decision-making government organizations for monitoring the infrastructural development activities and impose strict rules for preserving the natural resources.
- xi. Climate change mitigation strategies by adopting decarbonization technologies, which will reduce CO₂ emissions, such as renewable energy, fuel switching, energy efficiency improvements, and carbon capture, storage, and utilization.

Conclusion

Confounding variables such as urbanization and land use change may add uncertainty to the estimate of global temperature trends associated with climate change. This study estimated a significant increment of built-up area in the past 25 years by replacing other LULCs such as water bodies, agricultural and bare lands. The built-up area was increased from 1995 to 2015 by 158.22 km² (6.64%) to 386.74 km² (16.23%), whereas agricultural land was decreased significantly from 1461.92 km² (61.37%) to 926.14 km² (38.88%), respectively. The built-up area will be covered by 446.54 km² in 2030 and 512.83 km² in 2040, according to the LULC prediction. The maximum temperature was increased from 1995 to 2020 by 37.22 to 42.7 °C in summer with 1 °C standard deviations per 5 years and 22.18 °C to 28.94 °C in winter with 2 °C standard deviations per 5 years in the study region. Prediction states that the maximum LST will likely to be increased to 43.23 °C (2030) and 45.92 °C (2040) in summer, and 30.94 °C (2030) and 31.77 °C (2040) in winter. FGDs and KIIs assessments indicate that frequent LULC change was the main reason for increasing LSTs (71%), converts agricultural land and other green cover areas into infrastructure (69% very high), disrupts the hydrological cycle by increasing groundwater stress and reducing surface water bodies (51% very high), and ultimately causes flooding. In addition, 76% of experts agreed that heatwaves are the most influencing factors for adverse climate change, among other parameters. This study can be used as a framework for urban planners and policymakers in terms of participatory and sustainable rural–urban planning.

Although satellite data provide information that is not directly related to the quantitative rise of temperature records, in this work, local analyses of urban and global

warming-related issues were discussed by integration of remote sensing technology and primary traditional data collection system. Due to the fact that the study was conducted over a wide range of spatial scales, some ambiguity about the reliability of urban temperature records exists, which opens the way for future discussion on the impact of urban heating on climate data. Further progress in this area may benefit from the fresh views provided by novel methods and techniques, as well as from more research demonstrating the multi-scale effects of urbanization on the climate. Combining high-resolution data as nightlights, which has been enabled by advancements in remote sensing, statistical models, and ideas may offer an innovative approach for analyzing such problems.

Acknowledgements The authors would like to thank the US Geological Survey, Bangladesh Meteorological Department, Survey of Bangladesh, Ministry of Agriculture, Food Planning and Monitoring Unit of the Ministry of Food, Implementation Monitoring and Evaluation Division of Ministry of Planning, Bangladesh Bureau of Statistics, Rajshahi City Corporation and Rajshahi Development Authority for providing the relevant information. The authors like to express their gratitude to the participants of group discussions from different professional and community level. The authors would also like to thank the experts from Dynamic Institute of Geospatial Observation Network (DIGON) research and consultancy firm for proofreading the entire manuscript and doing language corrections.

Author contribution **Abdulla - Al Kafy and Abdullah-Al-Faisal**, conceived and designed the experiments, performed the experiments, analyzed and interpreted the data, contributed reagents, materials, analysis data, wrote the paper, proofreading the manuscript; **Abdullah Al Rakib and Kaniz Shaleha Akter**, contributed reagents, interpreted the data, materials, analyzed data, wrote the paper; **Zullyadini A Rahaman**, developed the revised study conduction idea by adding new datasets, contributed reagents, revised the paper and analyzed and interpreted the data and **Dewan Md. Amir Jahir, Gangaraju Subramanyam, Opelele Omeno Michel and Abhishek Bhatt**, help to collect the data from the field survey, revised the paper and interpreted the data in the revised manuscript.

Availability of data and material Not applicable.

Code availability Not applicable.

Declarations

Competing interests The authors declare no competing interests.

References

- Ahmed (2018) Assessment of urban heat islands and impact of climate change on socioeconomic over Suez Governorate using remote sensing and GIS techniques. *Egypt J Remote Sens Sp Sci* 21:15–25
- Ahmed B, Kamruzzaman M, Zhu X, Rahman M, Choi K (2013) Simulating land cover changes and their impacts on land surface temperature in Dhaka. *Bangladesh Remote Sens* 5:5969–5998
- Alamgir M, Khan N, Shahid S, Yaseen ZM, Dewan A, Hassan Q, Rasheed B (2020) Evaluating severity–area–frequency (SAF) of seasonal droughts in Bangladesh under climate change scenarios. *Stoch Environ Res Risk Assess* 1–18
- Al-Hamdan MZ, Oduor P, Flores AI, Kotikot SM, Mugo R, Ababu J, Farah H (2017) Evaluating land cover changes in Eastern and Southern Africa from 2000 to 2010 using validated Landsat and MODIS data. *Int J Appl Earth Obs Geoinf* 62:8–26
- Al sharif AAA, Pradhan B (2014) Monitoring and predicting land use change in Tripoli Metropolitan City using an integrated Markov chain and cellular automata models in GIS. *Arab J Geosci* 7:4291–4301
- Al-sharif AAA, Pradhan B (2015) A novel approach for predicting the spatial patterns of urban expansion by combining the chi-squared automatic integration detection decision tree, Markov chain and cellular automata models in GIS. *Geocarto Int* 30:858–881
- Al Rakib A, Akter KS, Rahman MN, Arpi S, Kafy A-A (2020a) Analyzing the pattern of land use land cover change and its impact on land surface temperature: a remote sensing approach in Mymensingh, Bangladesh. 1st Int. Student Res. Conf. 2020
- Al Rakib A, Ayan SM, Orthy TT, Sarker O, Intisar L, Arnob MA (2020b) In depth-analysis of urban resident-satisfaction level of Mirpur, Dhaka, Bangladesh: a participatory approach. 1st Int. Student Res. Conf. 2020
- Al Rakib A, Rahman MN, Arpi S, Ratu JF, Afroz F, Hossain N, Zubayer MS (2020c) An assessment on the housing satisfaction of Padma Residential Area, Rajshahi. 1st Int. Student Res. Conf. 2020
- Amzad Hossain M (2017) Financing small scale industries of Bangladesh with special reference to selected small industries in Rajshahi district
- Arsanjani JJ, Helbich M, Kainz W, Boloorani AD (2013) Integration of logistic regression, Markov chain and cellular automata models to simulate urban expansion. *Int J Appl Earth Obs Geoinf* 21:265–275
- Azari M, Tayyebi A, Helbich M, Reveshty MA (2016) Integrating cellular automata, artificial neural network, and fuzzy set theory to simulate threatened orchards: application to Maragheh. *Iran Geosci Remote Sens* 53:183–205
- Balogun IA, Ishola KA (2017) Projection of future changes in landuse/landcover using cellular automata/markov model over Akure city, Nigeria. *J Remote Sens Technol* 5:22–31
- Bank W (Ed.) (2016) Climate change & sustainable report- Bangladesh BBS (2013) District Statistics 2011. Ministry of Planning, Government of The People’s Republic of Bangladesh, Rajshahi
- Bonafoni S, Baldinelli G, Verducci P (2017) Sustainable strategies for smart cities: analysis of the town development effect on surface urban heat island through remote sensing methodologies. *Sustain Cities Soc* 29:211–218
- Celik B, Kaya S, Alganci U, Seker DZ (2019) Assessment of the relationship between land use/cover changes and land surface temperatures: a case study of thermal remote sensing. *FEB-FRESENIUS Environ Bull* 3:541
- Chakroborty S, Al Rakib A, Al Kafy A (2020) Monitoring water quality based on community perception in the Northwest Region of Bangladesh, in: 1st International Student Research Conference - 2020. Dhaka
- Chen XL, Zhao HM, Li PX, Yin ZY (2006) Remote sensing image-based analysis of the relationship between urban heat island and land use/cover changes. *Remote Sens Environ* 104:133–146
- Clemett A, Amin MM, Ara S, Akan MMR (2006) Background information for Rajshahi City. Bangladesh: WASPA Asia Project Report, p 2
- Connors JP, Galletti CS, Chow WTL (2013) Landscape configuration and urban heat island effects: assessing the relationship between

- landscape characteristics and land surface temperature in Phoenix. *Arizona Landsc Ecol* 28:271–283
- Dey NN, Al Rakib A, Kafy A-A, Raikwar V (2021) Geospatial modelling of changes in land use/land cover dynamics using multi-layer perception Markov chain model in Rajshahi City. *Bangladesh Environ Challenges* 4:100148. <https://doi.org/10.1016/j.envc.2021.100148>
- Djekic J, Mitkovic P, Dinic Brankovic M, Igic M, Djekic P, Mitkovic M (2018) The study of effects of greenery on temperature reduction in urban areas. *Therm Sci* 2018:122. <https://doi.org/10.2298/TSCI170530122D>
- Durand CP, Andalib M, Dunton GF, Wolch J, Pentz MA (2011) A systematic review of built environment factors related to physical activity and obesity risk: implications for smart growth urban planning. *Obes Rev* 12:e173–e182
- Eastman JR (2012) IDRISI selva manual and tutorial manual version 17. Worcester: MA Clark Univ, p 10
- Fahad MGR, Saiful Islam AKM, Nazari R, Alfi Hasan M, Tarekul Islam GM, Bala SK (2018) Regional changes of precipitation and temperature over Bangladesh using bias-corrected multi-model ensemble projections considering high-emission pathways. *Int J Climatol* 38:1634–1648
- Faisal A-A, Kafy A-A, Al Rakib A, Akter KS, Raikwar V, Jahir DMA, Ferdousi J, Kona MA (2021) Assessment and prediction of seasonal land surface temperature change using multi-temporal Landsat images and their impacts on agricultural yields in Rajshahi, Bangladesh. *Environ Challenges* 4:100147. <https://doi.org/10.1016/j.envc.2021.100147>
- Fortin M, Boots B, Csillag F, Rimmel TK (2003) On the role of spatial stochastic models in understanding landscape indices in ecology. *Oikos* 102:203–212
- Fu P, Weng Q (2018) Responses of urban heat island in Atlanta to different land-use scenarios. *Theor Appl Climatol* 133:123–135
- Gaur A, Eichenbaum MK, Simonovic SP (2018) Analysis and modelling of surface Urban Heat Island in 20 Canadian cities under climate and land-cover change. *J Environ Manage* 206:145–157
- Ghosh P, Mukhopadhyay A, Chanda A, Mondal P, Akhand A, Mukherjee S, Nayak SK, Ghosh S, Mitra D, Ghosh T (2017) Application of cellular automata and Markov-chain model in geospatial environmental modeling—a review. *Remote Sens Appl Soc Environ* 5:64–77
- Gopal S, Woodcock C (1996) Remote sensing of forest change using artificial neural networks. *IEEE Trans Geosci Remote Sens* 34:398–404
- Guan D, Li H, Inohae T, Su W, Nagaie T, Hokao K (2011) Modeling urban land use change by the integration of cellular automaton and Markov model. *Ecol Modell* 222:3761–3772
- Habitat UN (2016) Urbanization and development: emerging futures. *World Cities Rep* 3:4–51
- Halmy MWA, Gessler PE, Hicke JA, Salem BB (2015) Land use/land cover change detection and prediction in the north-western coastal desert of Egypt using Markov-CA. *Appl Geogr* 63:101–112
- Handayanto RT, Kim SM, Tripathi NK (2017) Land use growth simulation and optimization in the urban area, in: 2017 Second International Conference on Informatics and Computing (ICIC). IEEE, pp. 1–6
- Hart MA, Sailor DJ (2009) Quantifying the influence of land-use and surface characteristics on spatial variability in the urban heat island. *Theor Appl Climatol* 95:397–406
- Hu Z, Lo CP (2007) Modeling urban growth in Atlanta using logistic regression. *Comput Environ Urban Syst* 31:667–688
- IPCC (2014) Mitigation of climate change. *Contrib Work Gr III to Fifth Assess Rep Intergov Panel Clim Chang* 1454
- Islam M, Hassan M (2012) Land use changing pattern and challenges for agricultural land: a study on Rajshahi District. *J Life Earth Sci* 6. <https://doi.org/10.3329/jles.v6i0.9724>
- Islam K, Rahman MF, Jashimuddin M (2018) Modeling land use change using cellular automata and artificial neural network: the case of Chunati Wildlife Sanctuary. *Bangladesh Ecol Indic* 88:439–453
- Kafy A-A, Rahman MN, Al Rakib A, Arpi S, Faisal A-A (2019) Assessing satisfaction level of urban residential area: a comparative study based on resident's perception in Rajshahi City, Bangladesh, in: 1st International Conference on Urban and Regional Planning, Bangladesh. Dhaka: Bangladesh Institute of Planners, pp. 225–235
- Kafy A-A, Faisal A-A, Sikdar S, Hasan M, Rahman M, Khan MH, Islam R (2020a) Impact of LULC changes on LST in Rajshahi District of Bangladesh: a remote sensing approach. *J Geogr Stud* 3:11–23. <https://doi.org/10.21523/gcj5.19030102>
- Kafy A-A, Rahman MS, Al Faisal A, Hasan MM, Islam M (2020b) Modelling future land use land cover changes and their impacts on land surface temperatures in Rajshahi, Bangladesh. *Remote Sens Appl Soc Environ*. <https://doi.org/10.1016/j.rsase.2020.100314>
- Kafy A-A, Rahman MS, Islam M, Al Rakib A, Islam MA, Khan MHH, Sikdar MS, Sarker MHS, Mawa J, Sattar GS (2020c) Prediction of seasonal urban thermal field variance index using machine learning algorithms in Cumilla. Bangladesh. *Sustain Cities Soc* 64:102542. <https://doi.org/10.1016/j.scs.2020.102542>
- Kafy A-A, Al Rakib A, Akter KS, Rahaman ZA, Faisal A-A, Mallik S, Nasher NMR, Hossain MI, Ali MY (2021a) Monitoring the effects of vegetation cover losses on land surface temperature dynamics using geospatial approach in Rajshahi city, Bangladesh. *Environ Challenges* 100187. <https://doi.org/10.1016/j.envc.2021.100187>
- Kafy A-A, Faisal A-A, Raikwar V, Al Rakib A, Kona MA, Ferdousi J (2021b) Geospatial approach for developing an integrated water resource management plan in Rajshahi, Bangladesh. *Environ Challenges* 4:100139. <https://doi.org/10.1016/j.envc.2021.100139>
- Kafy A-A, Islam M, Sikdar MS, Ashrafi TJ, Al Faisal A, Islam MA, Al Rakib A, Khan MHH, Sarker MHS, Ali MY (2021c) Remote sensing-based approach to identify the influence of land use/land cover change on the urban thermal environment: a case study in Chattogram City, Bangladesh, in: Singh, R. (Ed.), *Re-Envisioning Remote Sensing Applications: Perspective from Developing Countries*. Taylor & Francis, pp. 216–237. <https://doi.org/10.1201/9781003049210-16>
- Kafy A-A, Naim MNH, Khan MHH, Islam MA, Al Rakib A, Faisal A-A, Sarker MHS (2021d) Prediction of urban expansion and identifying its impacts on the degradation of agricultural land: a machine learning-based remote-sensing approach in Rajshahi, Bangladesh, in: Singh, R. (Ed.), *Re-Envisioning Remote Sensing Applications: Perspective from Developing Countries*. Taylor & Francis, pp. 85–106. <https://doi.org/10.1201/9781003049210-6>
- Kafy A-A, Naim MNH, Subramanyam G, Faisal A-A, Ahmed NU, Al Rakib A, Kona MA, Sattar GS (2021e) Cellular automata approach in dynamic modeling of land cover changes using RapidEye images in Dhaka, Bangladesh. *Environ Challenges* 100084
- Lai L-W, Cheng W-L (2010) Urban heat island and air pollution—an emerging role for hospital respiratory admissions in an urban area. *J Environ Health* 72:32–36
- Lilly Rose A, Devadas MD (2009) Analysis of land surface temperature and land use/land cover types using remote sensing imagery - a case in Chennai City, India. *Seventh Int Conf Urban Clim*
- Liu G, Jin Q, Li J, Li L, He C, Huang Y, Yao Y (2017) Policy factors impact analysis based on remote sensing data and the CLUE-S model in the Lijiang River Basin, China. *CATENA* 158:286–297
- Losiri C, Nagai M, Ninsawat S, Shrestha RP (2016) Modeling urban expansion in Bangkok Metropolitan region using demographic-economic data through cellular automata-Markov Chain and multi-Layer perceptron-Markov chain models. *Sustainability* 8:686

- Lu Y, Wu P, Ma X, Li X (2019) Detection and prediction of land use/land cover change using spatiotemporal data fusion and the Cellular Automata–Markov model. *Environ Monit Assess* 191:68
- Maduako I, Ebinne E, Zhang Y, Basse P (2016a) Prediction of land surface temperature (LST) changes within Ikom City in Nigeria using artificial neural network (ANN). *Int J Remote Sens Appl* 6:96. <https://doi.org/10.14355/ijrsa.2016.06.010>
- Maduako ID, Yun Z, Patrick B (2016b) Simulation and prediction of land surface temperature (LST) dynamics within Ikom City in Nigeria using artificial neural network (ANN). *J Remote Sens GIS* 5:1–7
- Maimaitiyiming M, Ghulam A, Tiyp T, Pla F, Latorre-Carmona P, Halik Ü, Sawut M, Caetano M (2014) Effects of green space spatial pattern on land surface temperature: implications for sustainable urban planning and climate change adaptation. *J Photogramm Remote Sens* 89:59–66
- Maithani S (2015) Neural networks-based simulation of land cover scenarios in Doon valley. *India Geocarto Int* 30:163–185
- Mallick J, Kant Y, Bharath BD (2008) Estimation of land surface temperature over Delhi using Landsat-7 ETM+. *J Ind Geophys Union* 12:131–140
- Mansour S, Al-Belushi M, Al-Awadhi T (2020) Monitoring land use and land cover changes in the mountainous cities of Oman using GIS and CA-Markov modelling techniques. *Land Use Policy* 91:104414
- Mas JF, Flores JJ (2008) The application of artificial neural networks to the analysis of remotely sensed data. *Int J Remote Sens* 29:617–663
- Maulik U, Chakraborty D (2017) Remote Sensing Image Classification: a survey of support-vector-machine-based advanced techniques. *IEEE Geosci Remote Sens Mag* 5:33–52
- McCarthy MJ, Radabaugh KR, Moyer RP, Muller-Karger FE (2018) Enabling efficient, large-scale high-spatial resolution wetland mapping using satellites. *Remote Sens Environ* 208:189–201
- Mishra VN, Rai PK (2016) A remote sensing aided multi-layer perceptron-Markov chain analysis for land use and land cover change prediction in Patna district (Bihar). *India Arab J Geosci* 9:249
- Mishra VN, Rai PK, Prasad R, Punia M, Nistor M-M (2018) Prediction of spatio-temporal land use/land cover dynamics in rapidly developing Varanasi district of Uttar Pradesh, India, using geospatial approach: a comparison of hybrid models. *Appl Geomatics* 10:257–276
- Mozumder C, Tripathi NK (2014) Geospatial scenario based modelling of urban and agricultural intrusions in Ramsar wetland Deepor Beel in Northeast India using a multi-layer perceptron neural network. *Int J Appl Earth Obs Geoinf* 32:92–104
- Naim MNH, Kafy A-A (2021) Assessment of Urban Thermal Field Variance Index and defining the relationship between land cover and surface temperature in Chattogram city: A remote sensing and statistical approach. *Environ Challenges* 100107. <https://doi.org/10.1016/j.envc.2021.100107>
- Niyogi D (2019) Land surface processes, in: Current trends in the representation of physical processes in weather and climate models. Springer, pp. 349–370
- Nurwanda A, Honjo T (2020) The prediction of city expansion and land surface temperature in Bogor City, Indonesia. *Sustain Cities Soc* 52:101772
- Ogashawara I, Bastos VDSB (2012) A quantitative approach for analyzing the relationship between urban heat islands and land cover. *Remote Sens* 4:3596–3618
- Osgouei PE, Kaya S (2017) Analysis of land cover/use changes using Landsat 5 TM data and indices. *Environ Monit Assess* 189:136
- Pal S, Ziaul S (2017) Detection of land use and land cover change and land surface temperature in English Bazar urban centre. *Egypt J Remote Sens Sp Sci* 20:125–145
- Pontius RG Jr, Millones M (2011) Death to Kappa: birth of quantity disagreement and allocation disagreement for accuracy assessment. *Int J Remote Sens* 32:4407–4429
- Rahman M (2016) Detection of land use/land cover changes and urban sprawl in Al-Khobar, Saudi Arabia: an analysis of multi-temporal remote sensing data. *ISPRS Int J Geo-Information* 5:15
- Rahman KM, Melville L, Fulford D, Huq SMI (2017a) Green-house gas mitigation capacity of a small scale rural biogas plant calculations for Bangladesh through a general life cycle assessment. *Waste Manag Res* 35:1023–1033
- Rahman MT, Aldosary AS, Mortoja M (2017b) Modeling future land cover changes and their effects on the land surface temperatures in the Saudi Arabian eastern coastal city of Dammam. *Land* 6:36
- Rahman MS, Mohiuddin H, Kafy A-A, Sheel PK, Di L (2018) Classification of cities in Bangladesh based on remote sensing derived spatial characteristics. *J Urban Manag*
- RDA (2008) Working paper on Existing land use, demographic and transport (revised). Government of The People’s Republic of Bangladesh Ministry of Housing and Public Works
- Roy DP, Wulder MA, Loveland TR, Woodcock CE, Allen RG, Anderson MC, Helder D, Irons JR, Johnson DM, Kennedy R (2014) Landsat-8: science and product vision for terrestrial global change research. *Remote Sens Environ* 145:154–172
- Santé I, García AM, Miranda D, Crecente R (2010) Cellular automata models for the simulation of real-world urban processes: a review and analysis. *Landsc Urban Plan* 96:108–122
- Shatnawi N, Abu Qdais H (2019) Mapping urban land surface temperature using remote sensing techniques and artificial neural network modelling. *Int J Remote Sens* 1–16
- Singh SK, Mustak S, Srivastava PK, Szabó S, Islam T (2015) Predicting spatial and decadal LULC changes through cellular automata Markov chain models using earth observation datasets and geo-information. *Environ Process* 2:61–78
- Trolle D, Nielsen A, Andersen HE, Thodsen H, Olesen JE, Børgesen CD, Refsgaard JC, Sonnenborg TO, Karlsson IB, Christensen JP (2019) Effects of changes in land use and climate on aquatic ecosystems: coupling of models and decomposition of uncertainties. *Sci Total Environ* 657:627–633
- Ullah S, Ahmad K, Sajjad RU, Abbasi AM, Nazeer A, Tahir AA (2019a) Analysis and simulation of land cover changes and their impacts on land surface temperature in a lower Himalayan region. *J Environ Manage* 245:348–357
- Ullah S, Tahir AA, Akbar TA, Hassan QK, Dewan A, Khan AJ, Khan M (2019b) Remote sensing-based quantification of the relationships between land use land cover changes and surface temperature over the lower Himalayan region. *Sustainability* 11:5492
- UN-DESA (2018) World urbanization prospects: the 2018 revision, Online Edition
- UN (2019) Bangladesh population, Rajshahi [WWW Document]
- UN “Sustainable Development Goals” (2015) UN, “Sustainable Development Goals,” 2015 [WWW Document]
- Van Gerven M, Bohte S (2017) Artificial neural networks as models of neural information processing. *Front Comput Neurosci* 11:114
- Verburg PH, Van De Steeg J, Veldkamp A, Willemsen L (2009) From land cover change to land function dynamics: a major challenge to improve land characterization. *J Environ Manage* 90:1327–1335
- Wadud MA (2018) Industrialization in Northwest Bangladesh. Ph. D. Thesis, Rajshahi: University of Rajshahi

- Wang H, Zhang Y, Tsou JY, Li Y (2017) Surface urban heat island analysis of Shanghai (China) based on the change of land use and land cover. *Sustainability* 9:1538
- Yang C, He X, Yan F, Yu L, Bu K, Yang J, Chang L, Zhang S (2017) Mapping the influence of land use/land cover changes on the urban heat island effect—a case study of Changchun, China. *Sustainability* 9:312
- Zhou W, Huang G, Cadenasso ML (2011) Does spatial configuration matter? Understanding the effects of land cover pattern on land surface temperature in urban landscapes. *Landsc Urban Plan* 102:54–63
- Zine El Abidine EM, Mohieldeen YE, Mohamed AA, Modawi O, Al-Sulaiti MH (2014) Heat wave hazard modelling: Qatar case study. *Q Sci Connect* 9